Toward the helium abundance: The behavior of the helium 10830Å in the open cluster Stock 2 and field stars

Mingjie Jian (简明杰) @ Department of Astronomy, Stockholm University

Xiaoting Fu (符晓婷), Noriyuki Matsunaga (松永典之), Valentina D'Orazi, Angela Bragaglia, Daisuke Taniguchi (谷口大輔), Min Fang (房敏), Nicoletta Sanna, Sara Lucatello, Antonio Frasca, Javier Alonso-Santiago, Giovanni Catanzaro, Ernesto Oliva, and the WINERED team

Stellar nucleosynthesis

- Helium and heavier elements are enriched in the "material cycle".
- The next generation stars are born with enriched chemical compositions:
  - Y, Z: mass ratio of helium and heavier elements of a star.

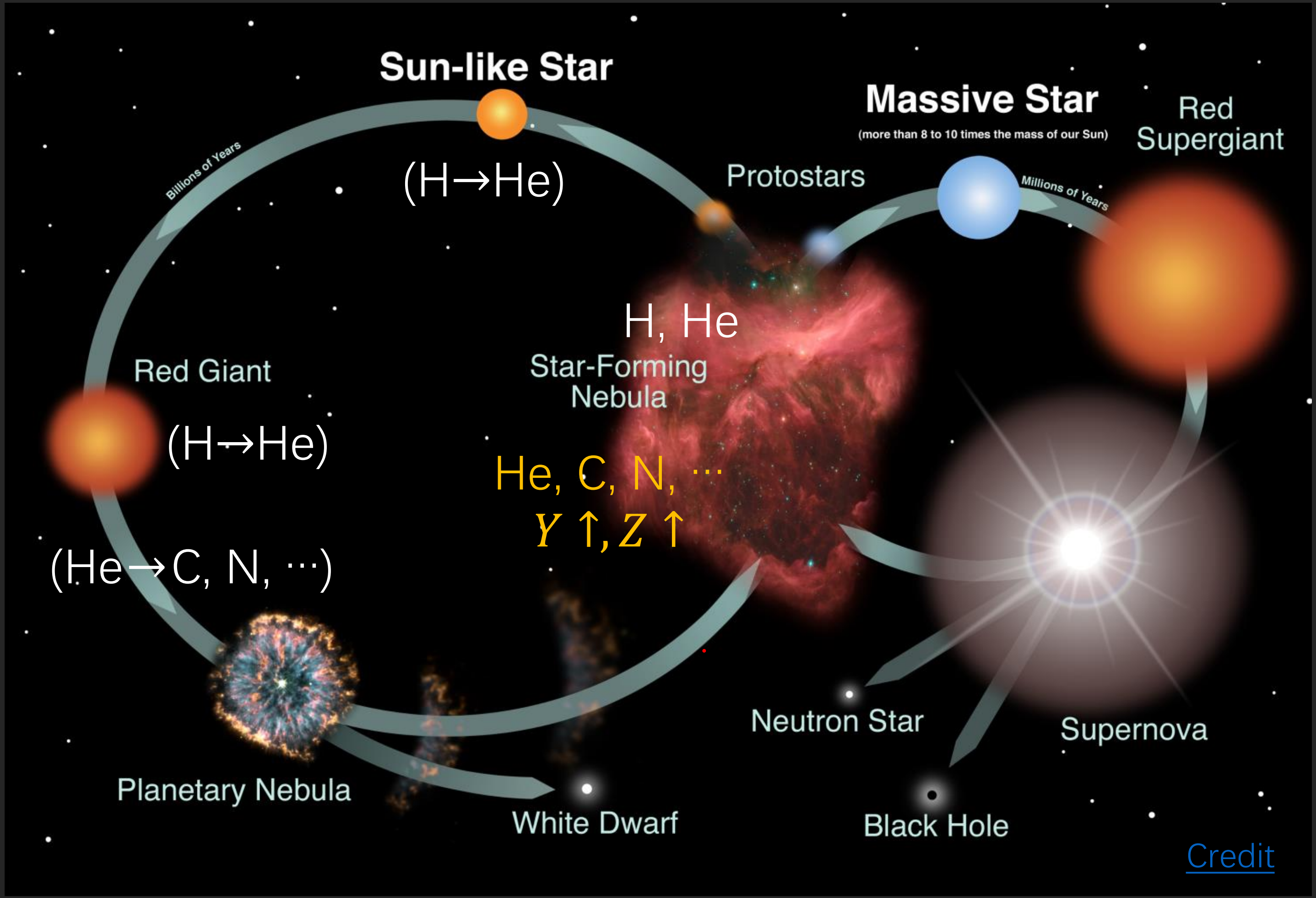

The elements being measured

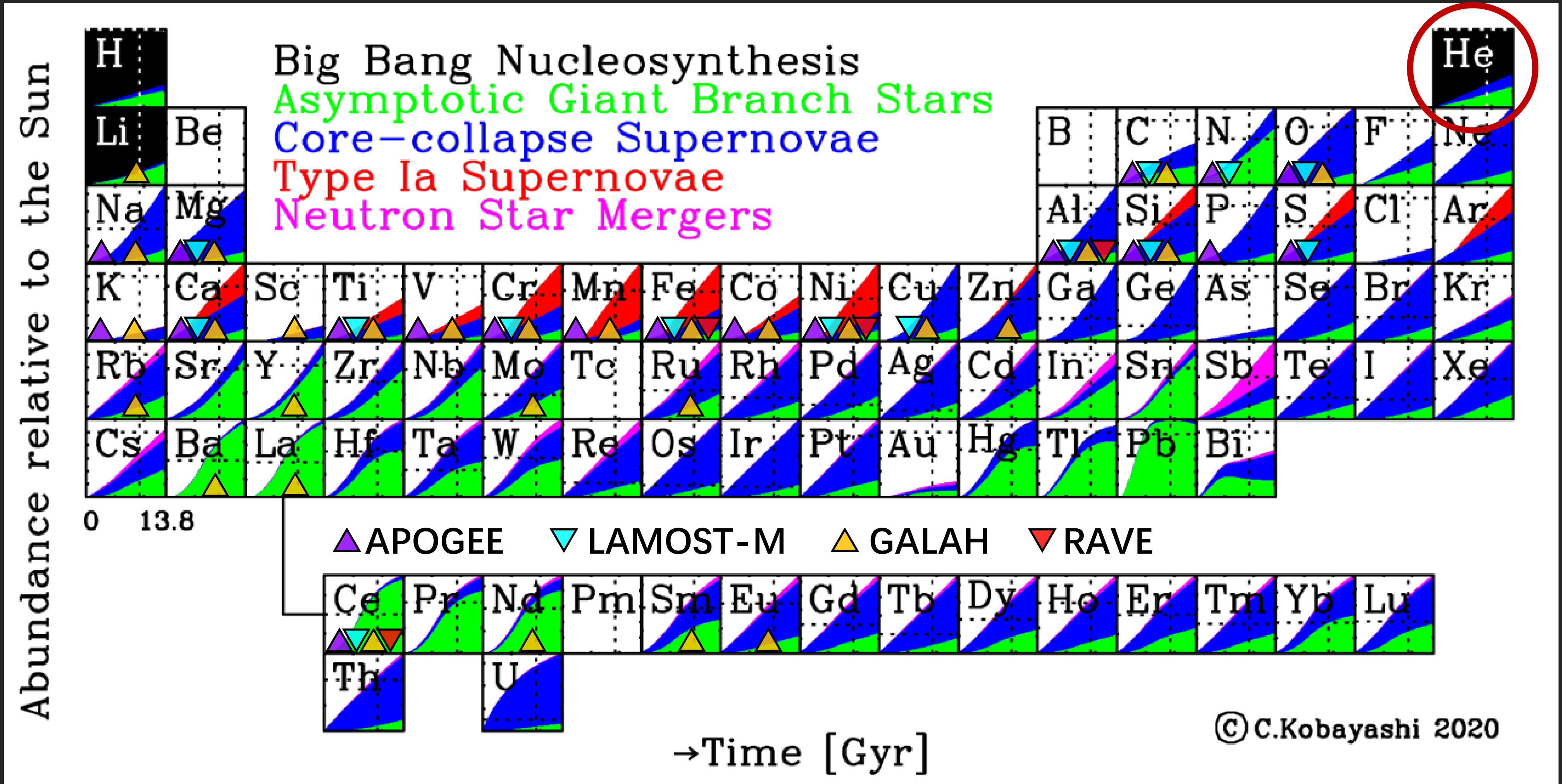

Mg – Fe vs Y – Z diagram

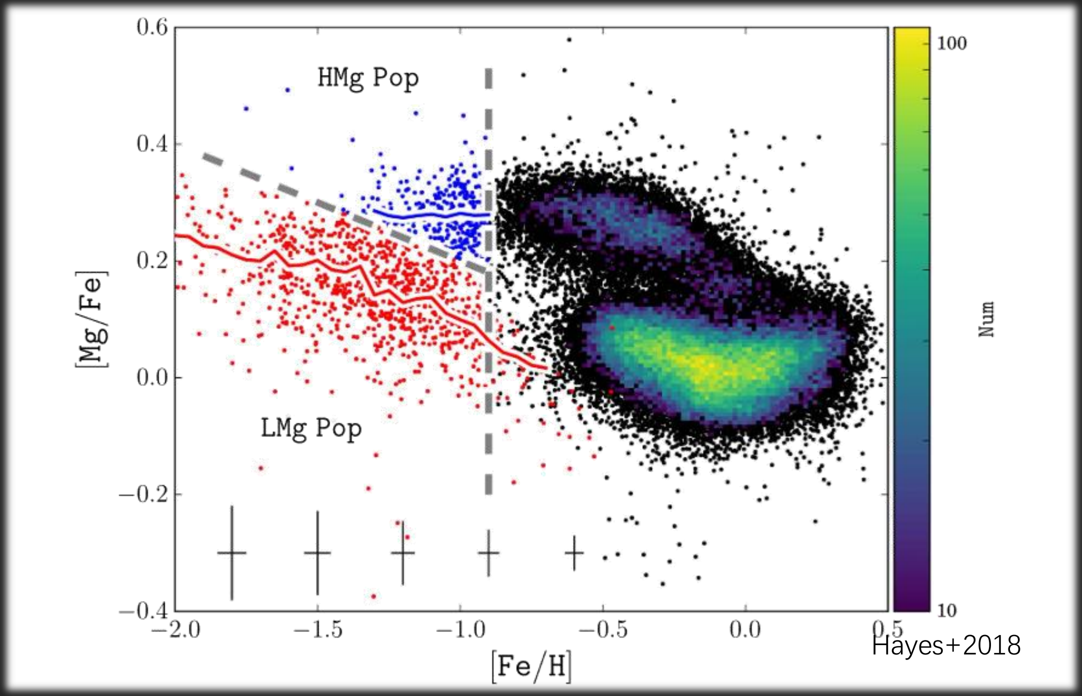

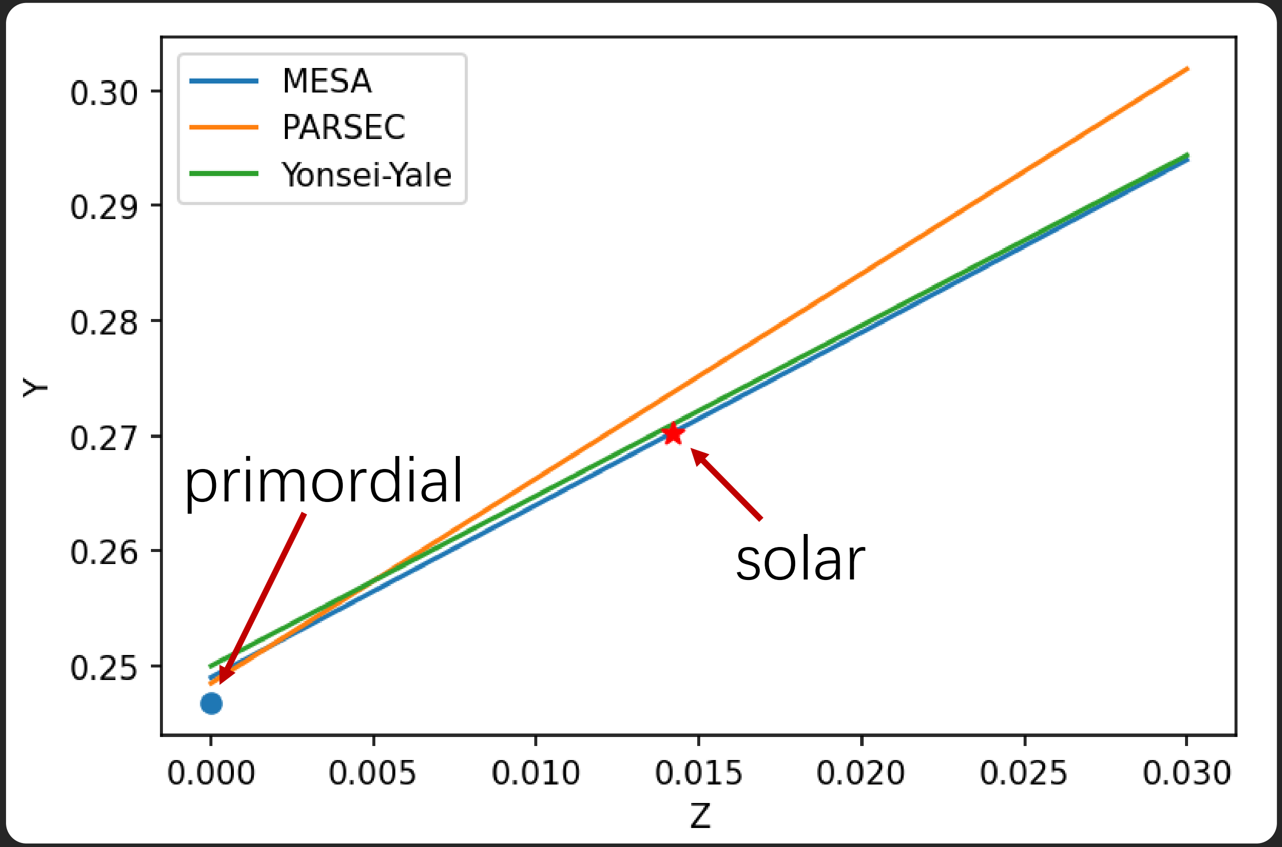

Universal helium enrichment law?

No!

- Linear relation fitted by primordial and solar Y, Z.
- Globular clusters:
  - Y variation
- Asteroseismology:
  - smaller slope

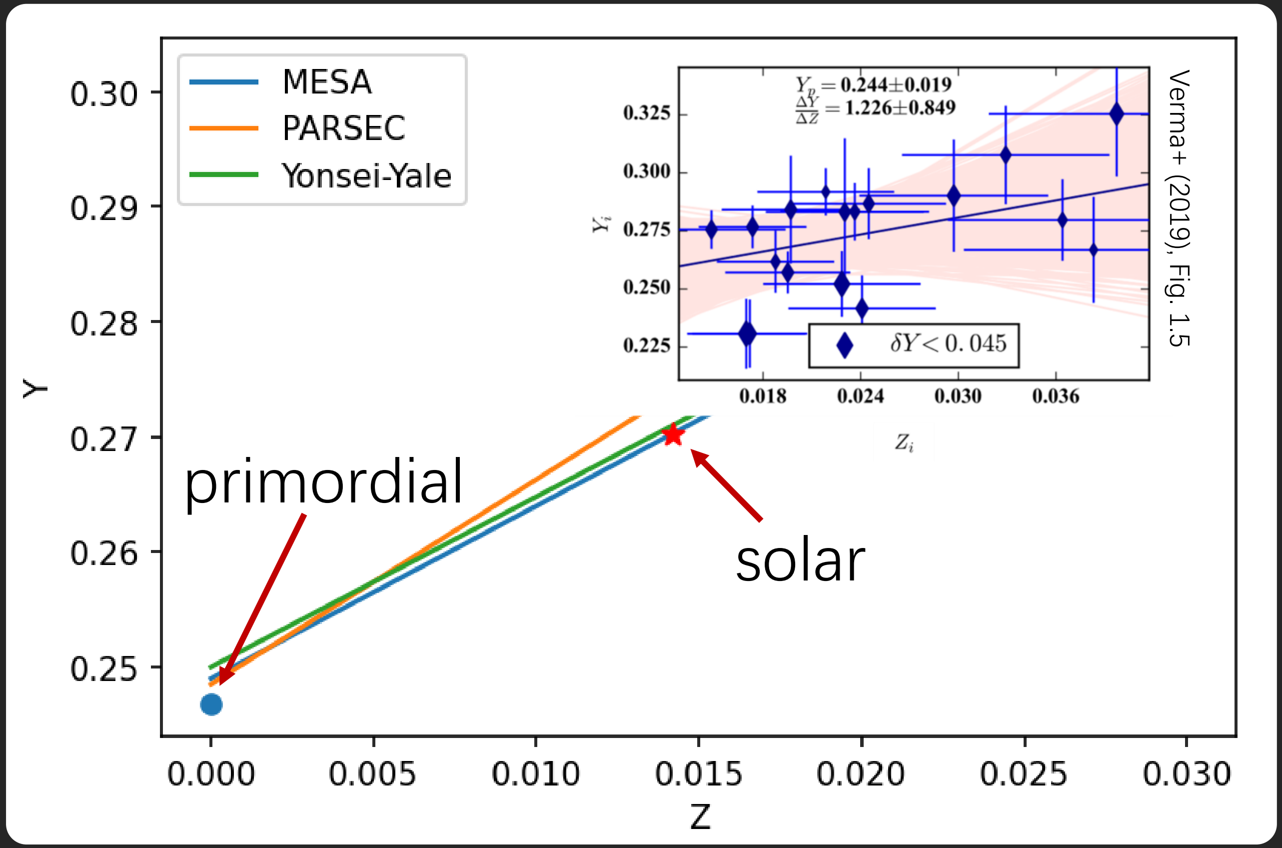

He energy levels

- Resonance lines:
  - In UV wavelength
  - Weak in FGK type stars
- He 10830
  - Present in most late-type stars and formed in the chromosphere.
  - Formation mechanisms:
    - Photoionization Recombination (PR), triggered by high-energy photons from the corona.
    - Collisional Excitation (CE)

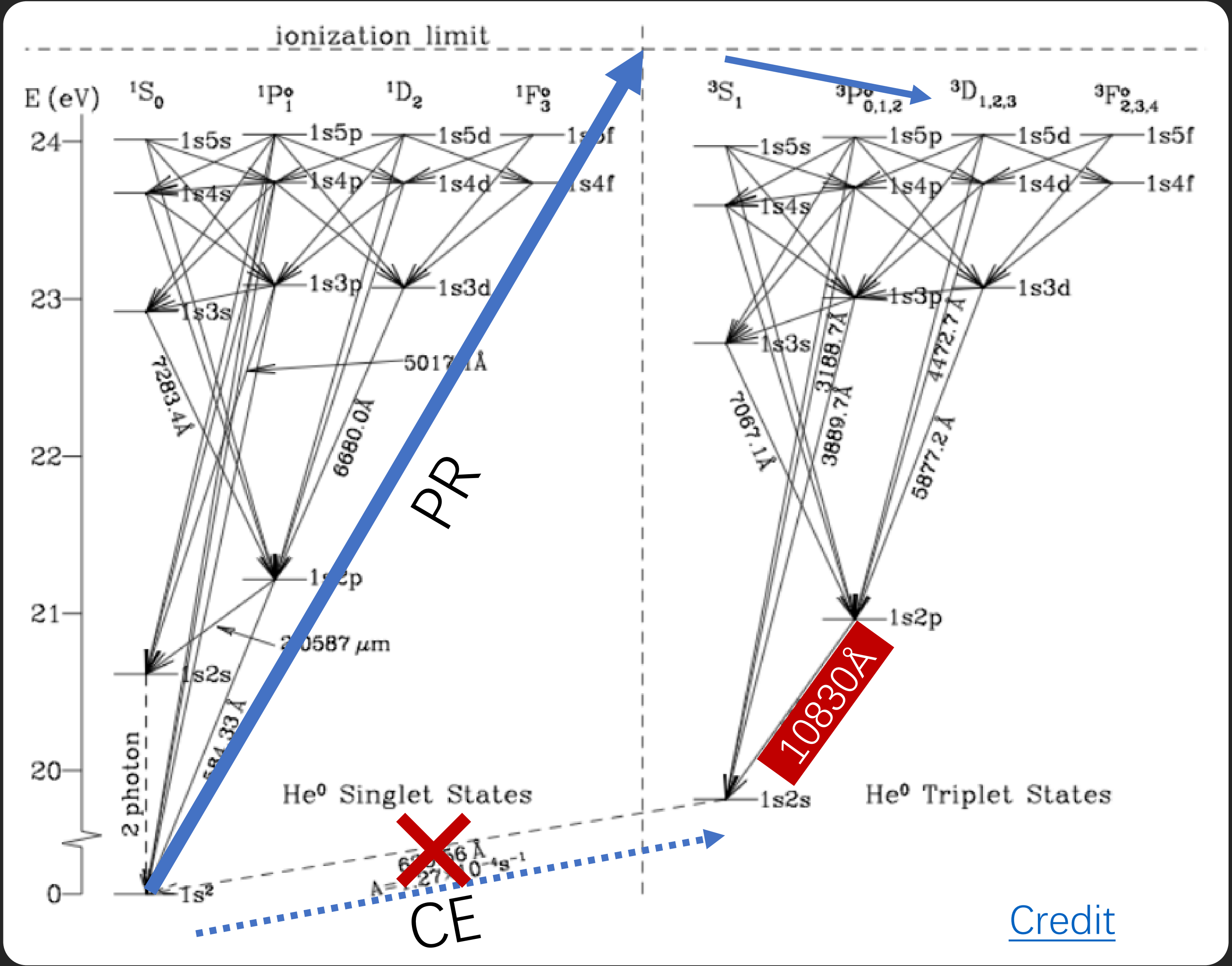

Credit

Target line: The He 10830

- He 10830 is a helium absorption feature which appears in most of the late-type stars' spectra.
- Near infrared: suffers less extinction.

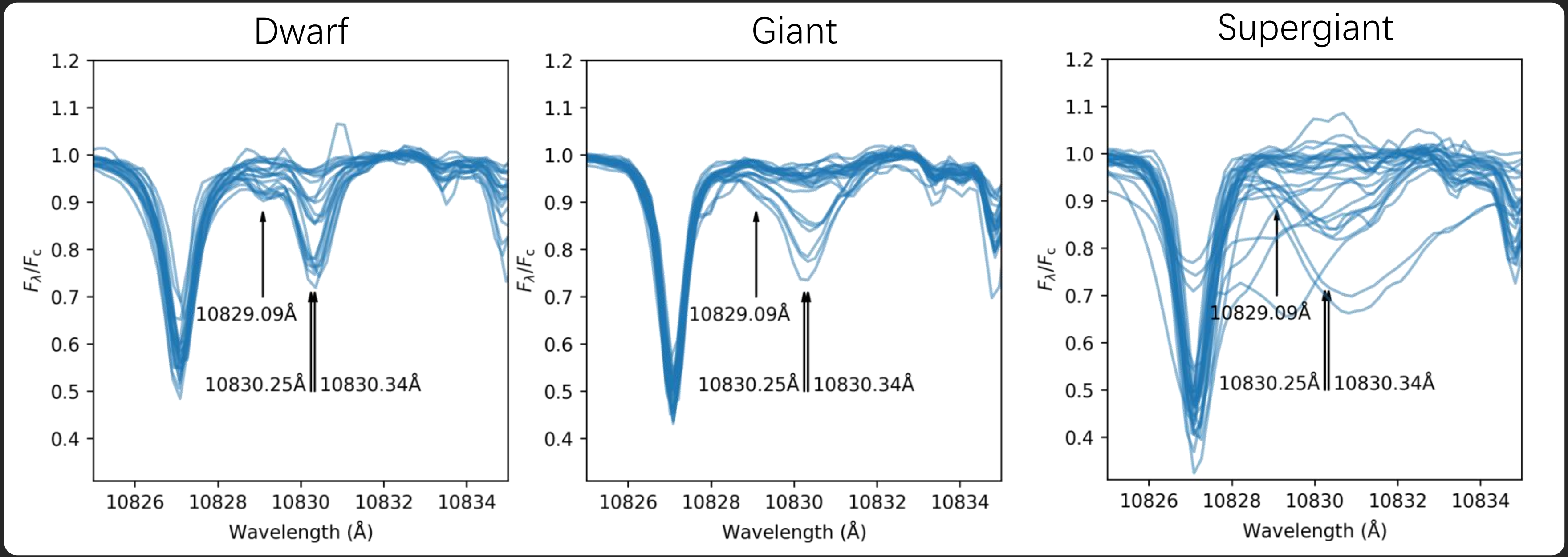

→ Y?

EW(He) – spectral type trend

Observations before 1990s

- Zirin (1982)

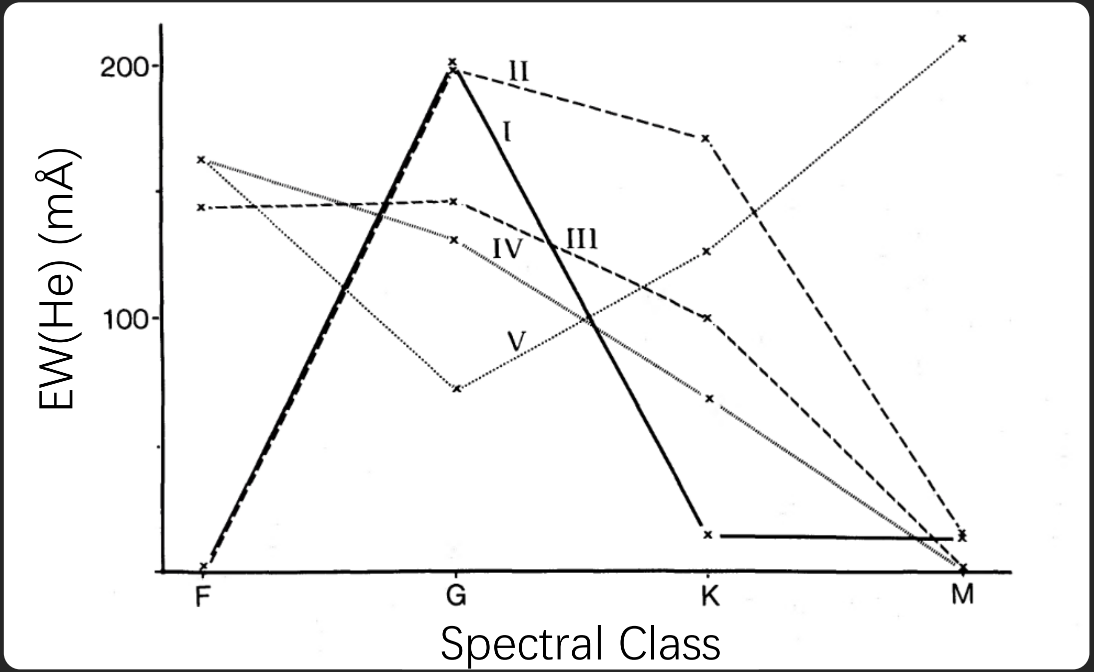

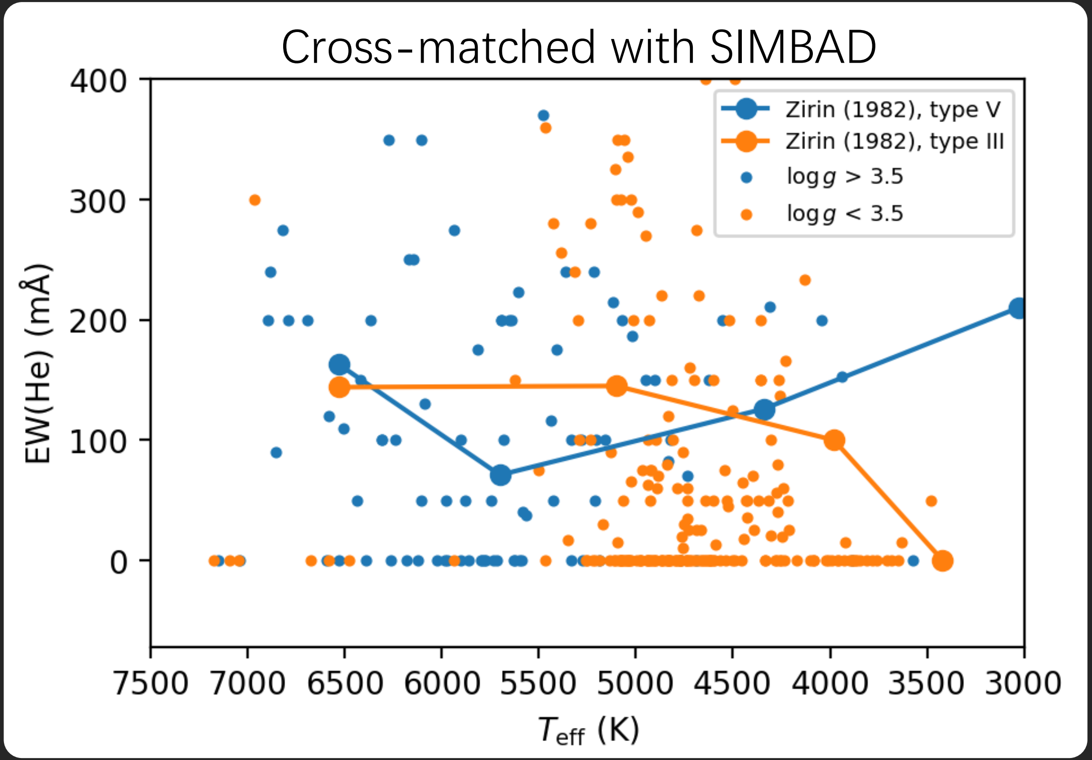

- Only rough trends were derived.

EW(He) – T_{eff} trend

Observations after 1990s

- Most of the stars are metal-poor except for those from Fuhrmeister+(2020).
- No clear trend is found except for the M-dwarfs.
- A new sample of stars with similar surface helium abundance is necessary.

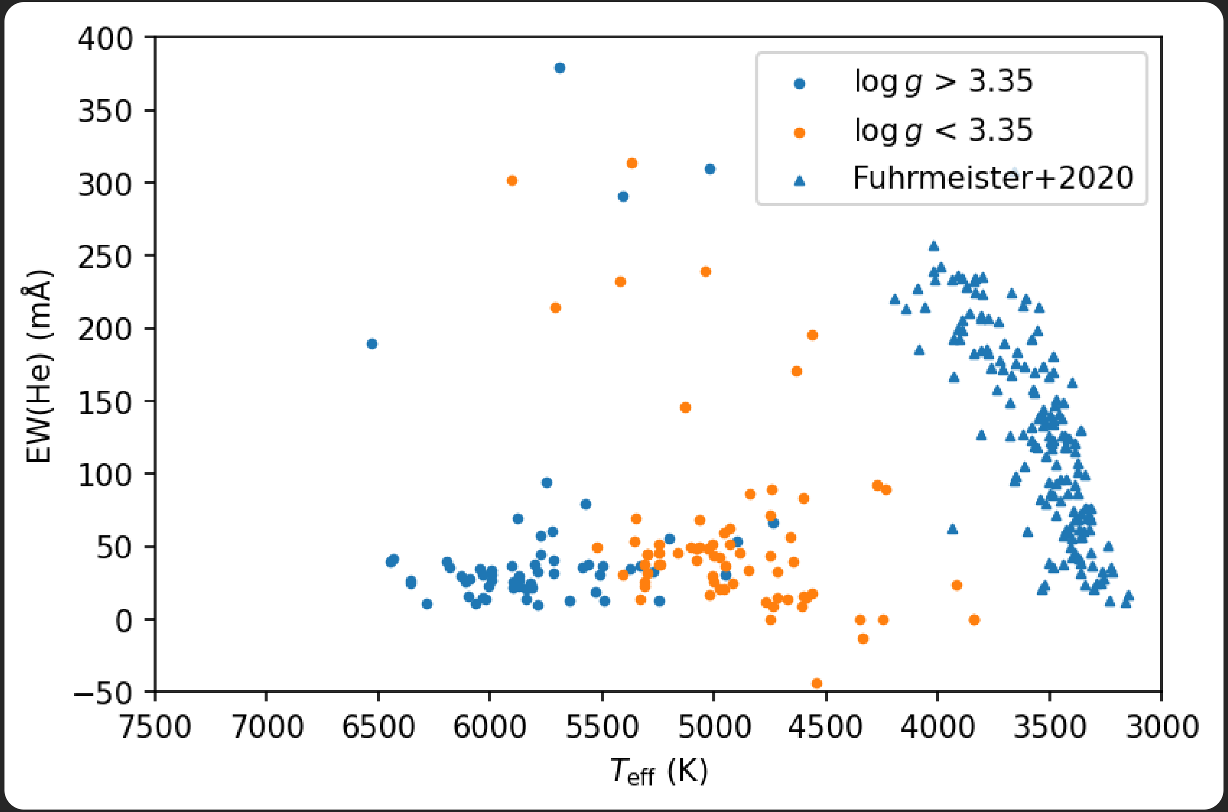

Connection with formation mechanisms

- Previous works suggest EW(He) are correlated with both $\log R'_{\mathrm{HK}}$ and $\log L_{\mathrm{X}}/L_{\mathrm{bol}}$.
- Can He 10830 be used to measure Y?

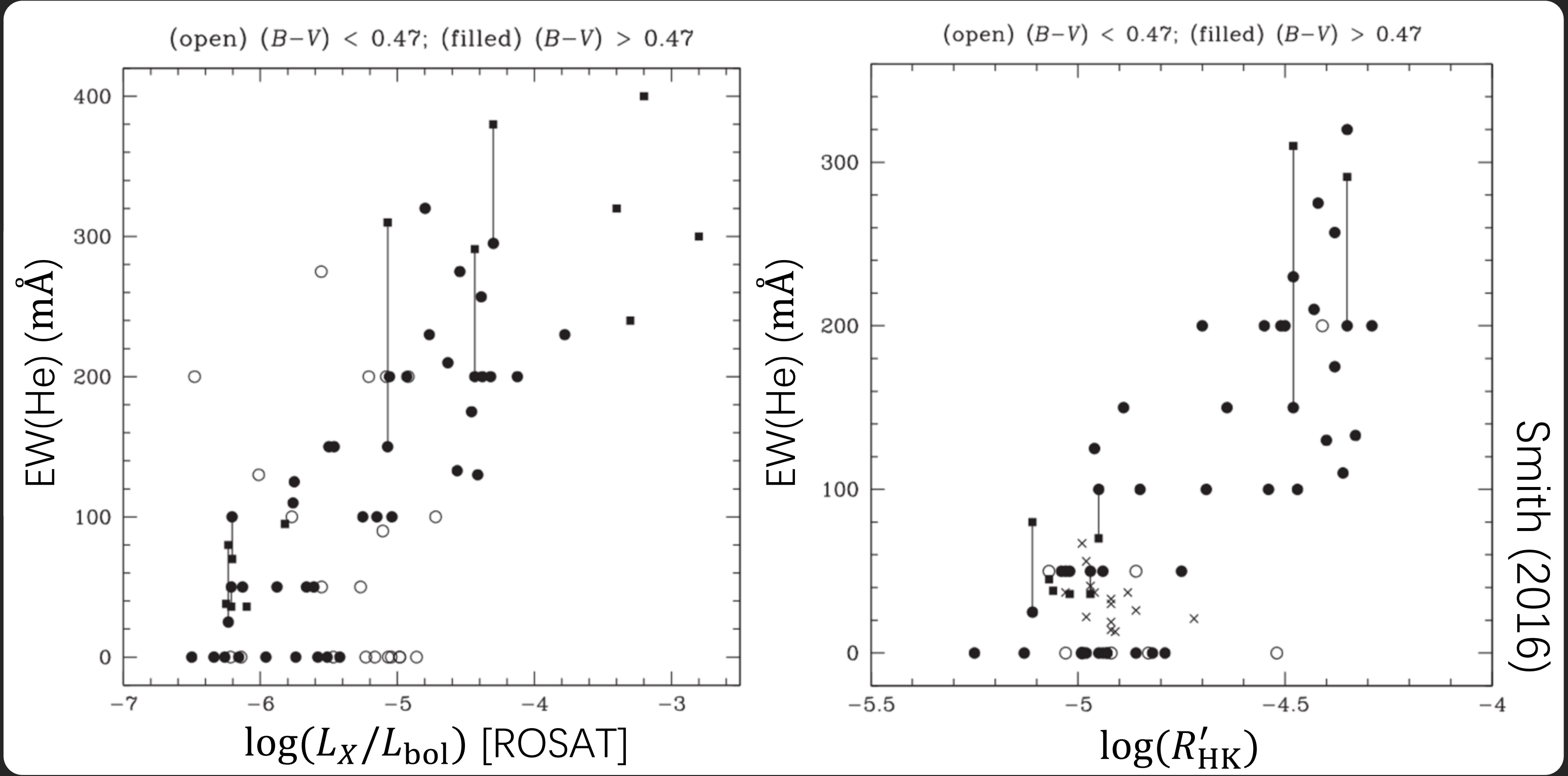

Smith (2016)

Stars with varied Y

(Y, $\log R'_{\mathrm{HK}}$, L_{X}, T_{eff}, $\log g$)

Stars with same Y, T_{eff}, $\log g$, [Fe/H]

Stock 2: an open cluster

- Single stellar population:
  - same age, similar chemical composition
- Age: 450Myr
- [Fe/H] = -0.07
- MSTO stellar mass: $\approx 2.8M_{\odot}$
  - (Alonso-Santiago+2021)

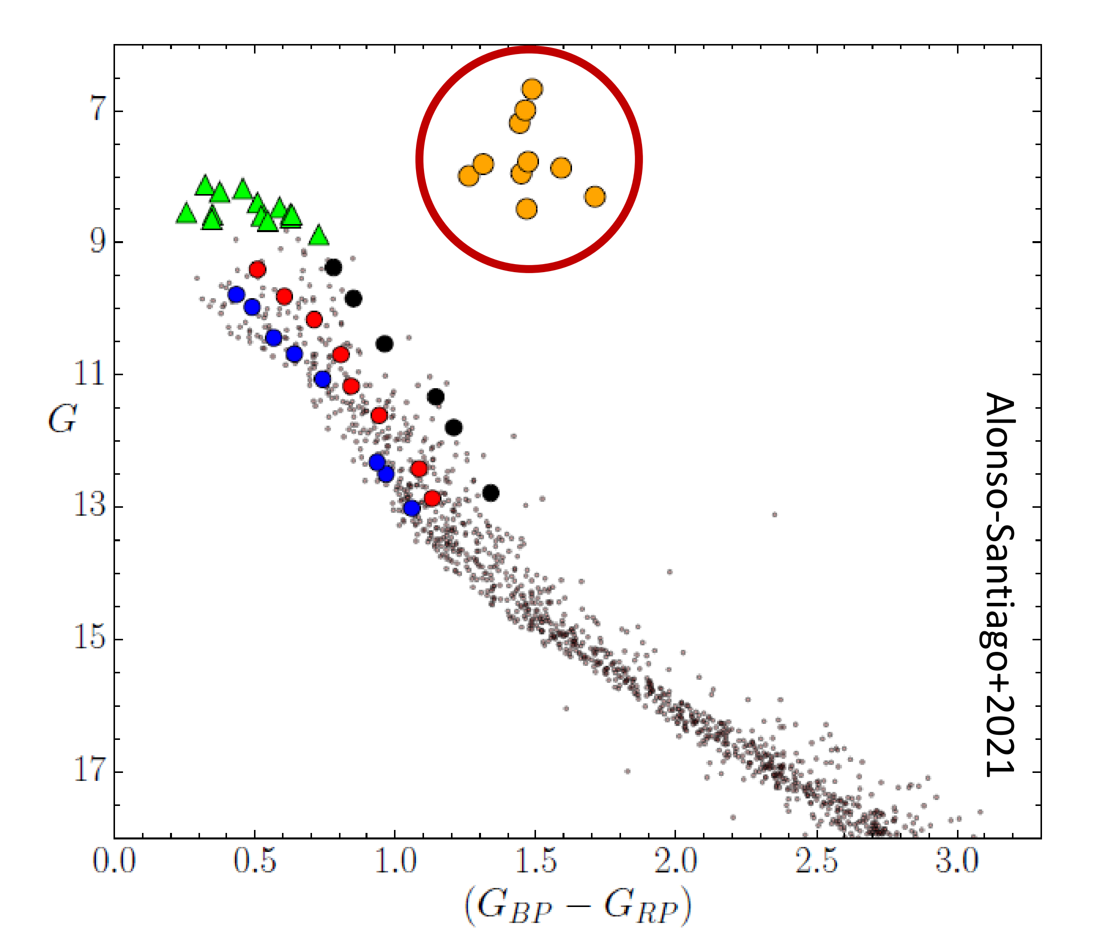

Credit

Red clump stars in Stock 2

- The Y in dwarfs:
  - Diffusion
  - First dredge-up
- The Y in RCs:
  - The Ys are similar
  - Their Ys are expected to be larger than those in main-sequence phase.

Isochrone

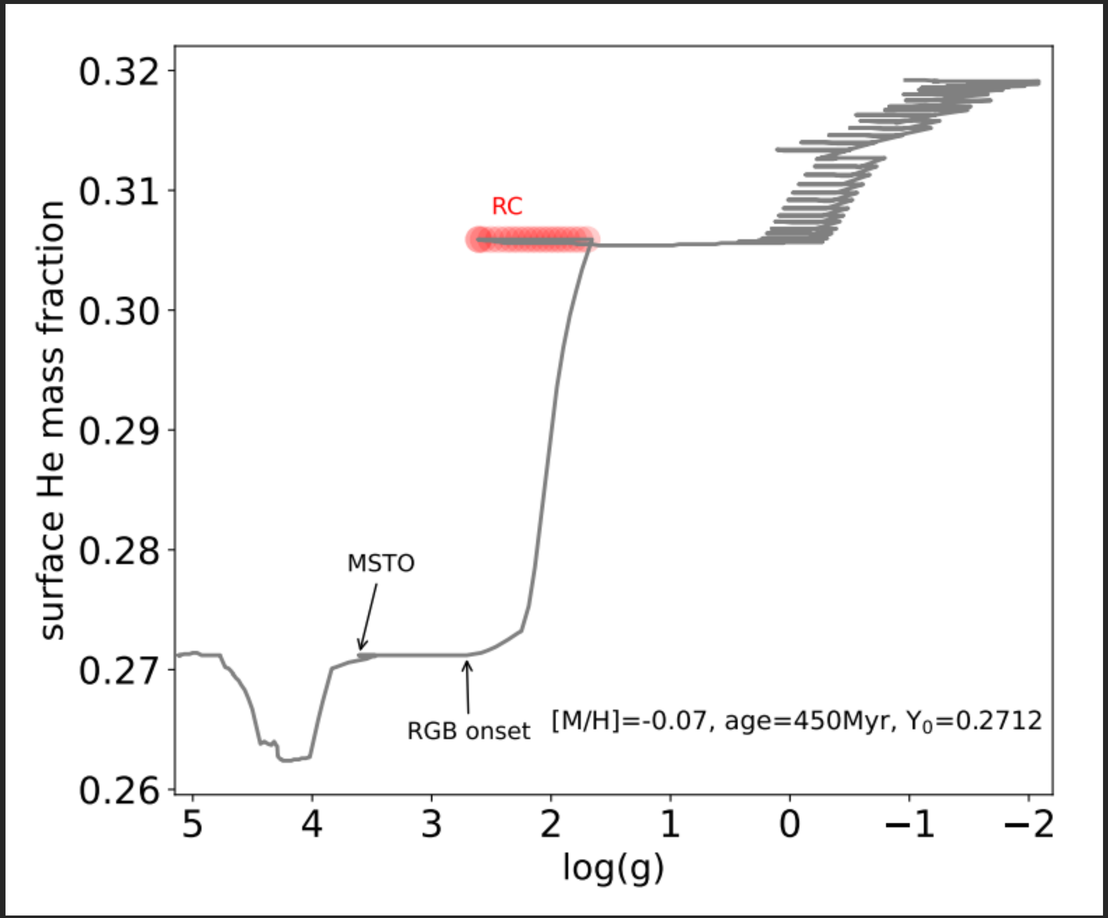

Observation

- Stellar Population Astrophysics
  - PI: L. Origlia
- High spectral resolution:
  - Probe detailed line shape
- Optical and NIR spectra in the same time
  - He 10830 + Ca II HK
  - Avoid temporal variation of He 10830 or Ca II HK lines.

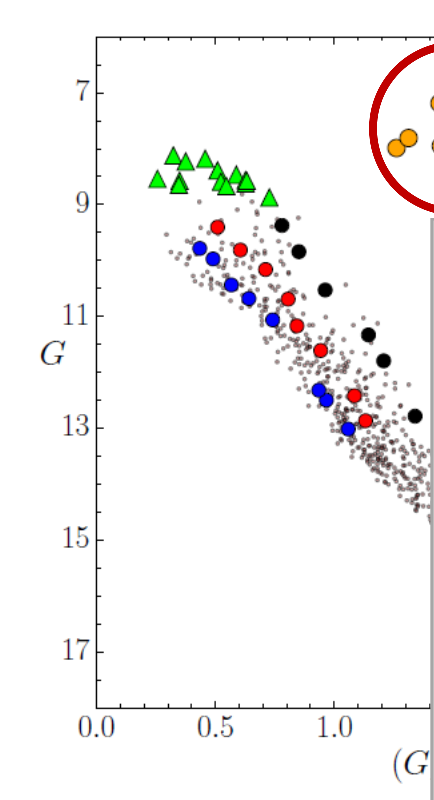

- Wavelength
  - 3870-6910Å + 9530-24230Å
- Resolution
  - 115,000 + 50,000
- Target
  - Open cluster Stock-2
  - 9 giants

Measurement of He 10830
1. blending

- Several weak atomic lines present around He 10830.
- The synthetic spectra are stronger than observed spectra.
- $\log gf$ values requires correction.

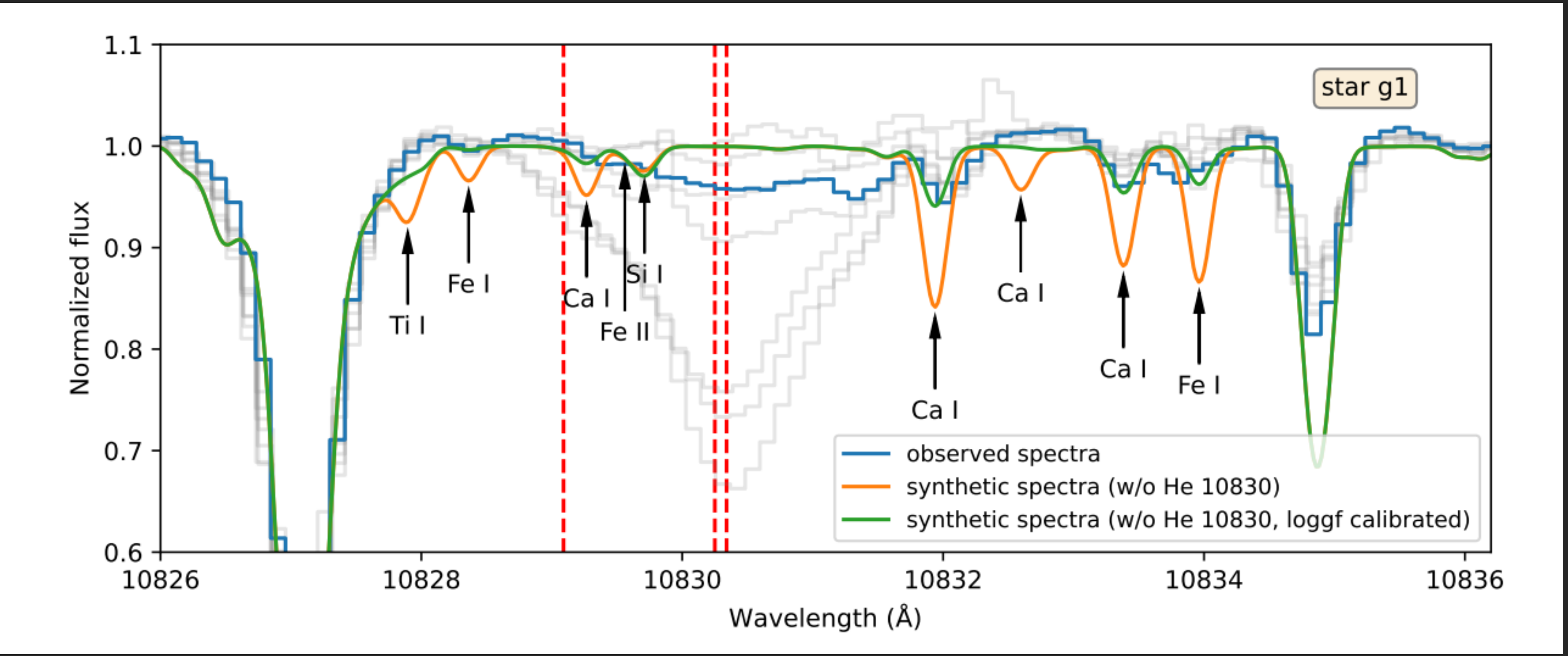

Measurement of He 10830

2. line fitting

- Si I and telluric: Voigt profile
- He features: skew Gaussian profile
  - $\frac{A}{\sigma\sqrt{2\pi}}\left\{1+\mathrm{erf}\left[\frac{\gamma(x-\mu)}{\sigma\sqrt{2\pi}}\right]\right\}\exp\left[-\frac{(x-\mu)^2}{2\sigma^2}\right]$

- A: amplitude
- μ: feature centre
- γ:asymmetry

- EW: equivalent width
- $\lambda_{\mathbf{peak}}$: peak wavelength
- B/R: blue-to-red ratio

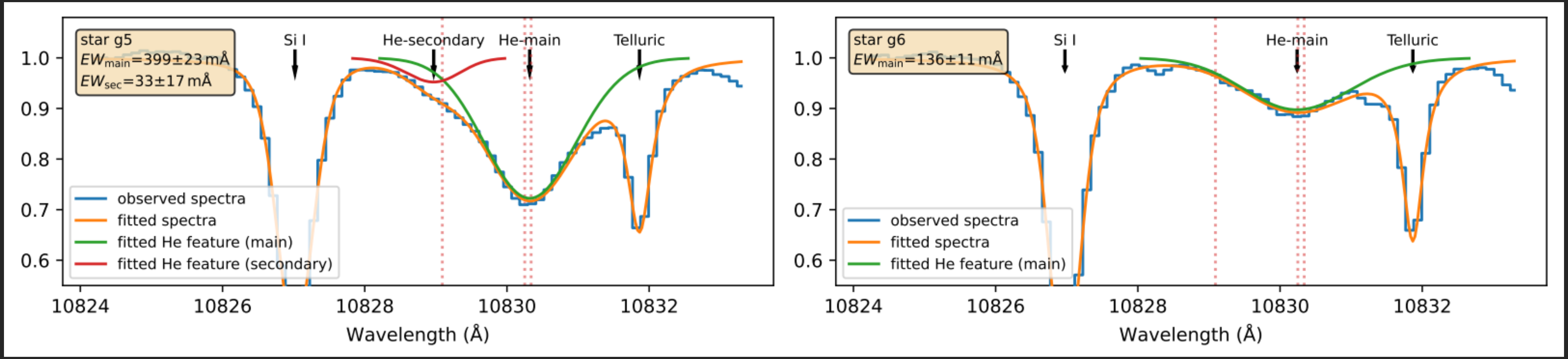

Measurement of Ca II HK lines

For constraining the chromospheric structure

- Measuring the core-emission of the Ca II lines.
- $\log R'_{\mathrm{HK}} = (F'_{\mathrm{K}} + F'_{\mathrm{H}})/\sigma T_{\mathrm{eff}}^4$

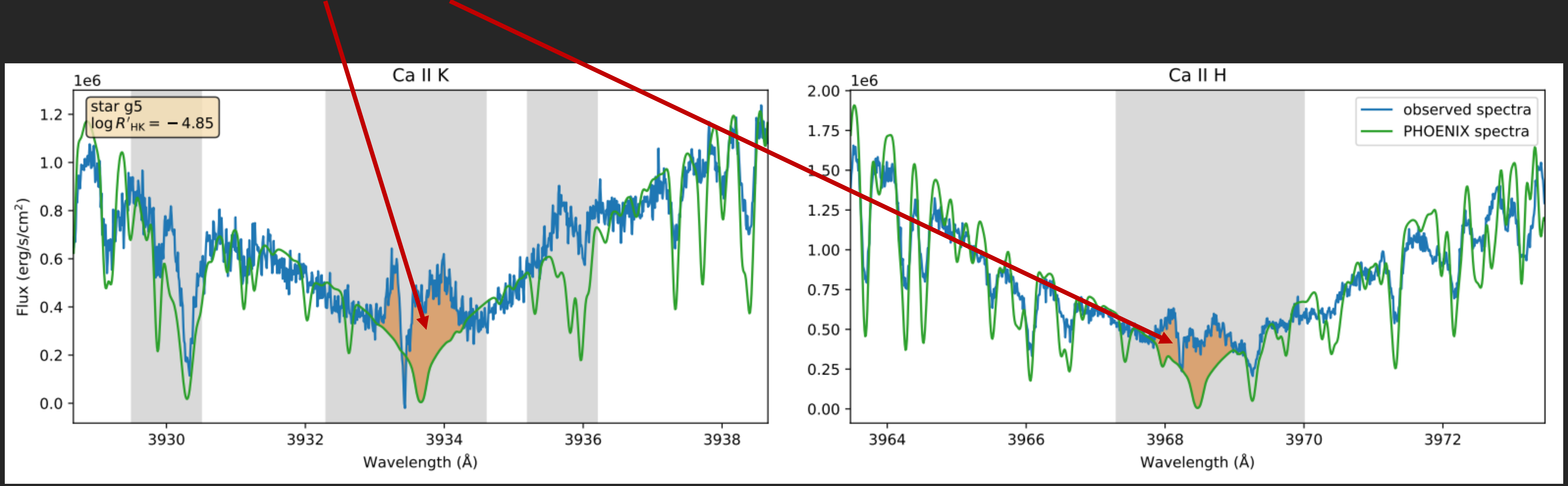

$\log R'_{\mathrm{HK}}$ - EW relation

- Linear relation between He 10830 EW and $\log R'_{\mathrm{HK}}$
  - For Stock 2 RCs and field dwarfs
- The EWs of RCs are larger than dwarfs ([Fe/H]~0).
- $Y_{\mathrm{RC}} > Y_{\mathrm{dwarf}}$
- $Y \uparrow \Rightarrow EW \uparrow$

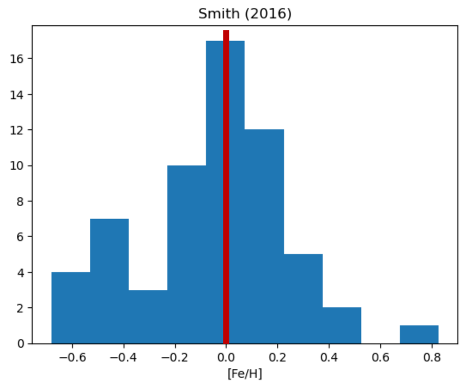

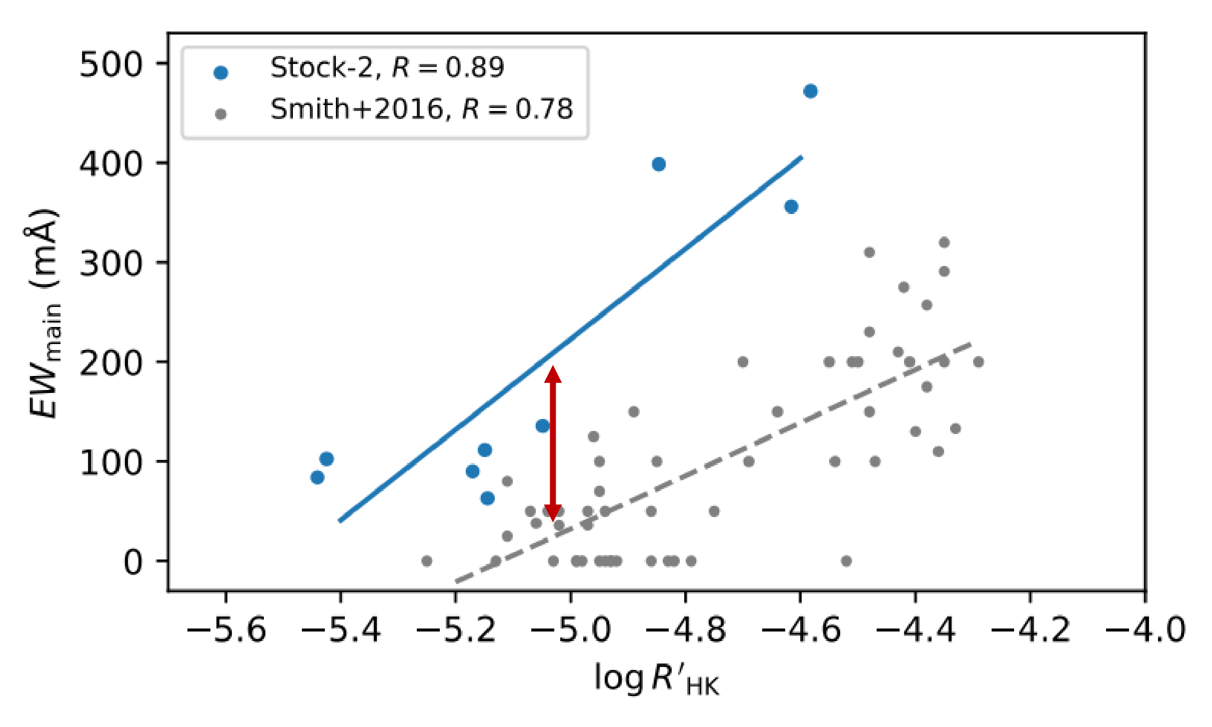

He 10830 in field stars:
Targets and observations

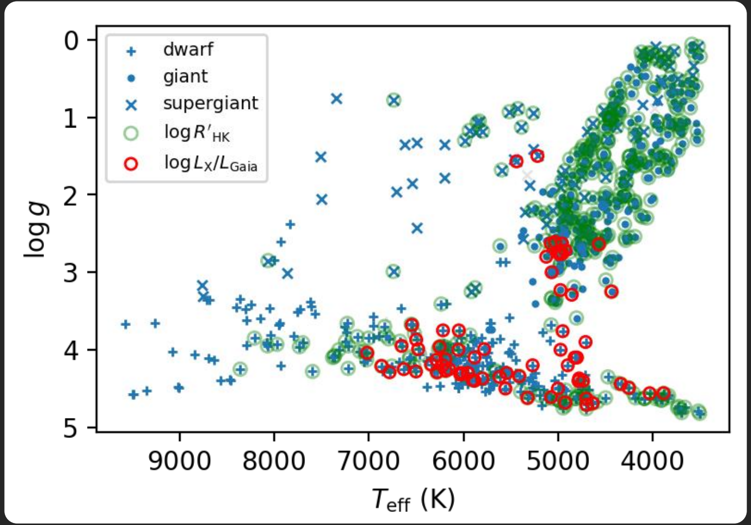

Field-WD

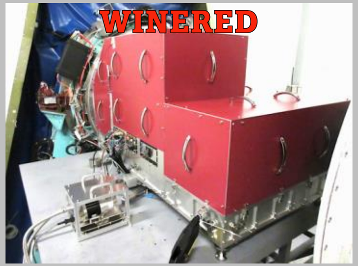

- Wavelength
  - 9100-13500Å
- Resolution
  - 28,000
- Target
  - AFGK type stars
  - 93 dwarfs, 70 giants, 29 supergiants
  - [Fe/H]: -1~0

Field-XSL

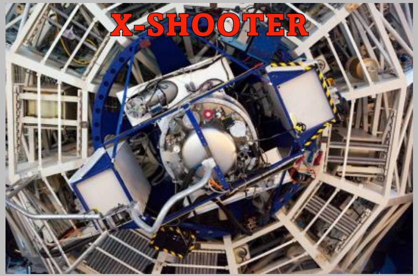

- Wavelength
  - 3000-24800Å
- Resolution
  - 10,000
- Target (X-shooter Spectral Library)
  - AFGK type stars
  - 225 dwarfs, 265 giants, 58 supergiants
  - [Fe/H]: -2~0

EW(He) – T_{eff} trend
of new targets

- More detailed trends compared with Zirin (1982)

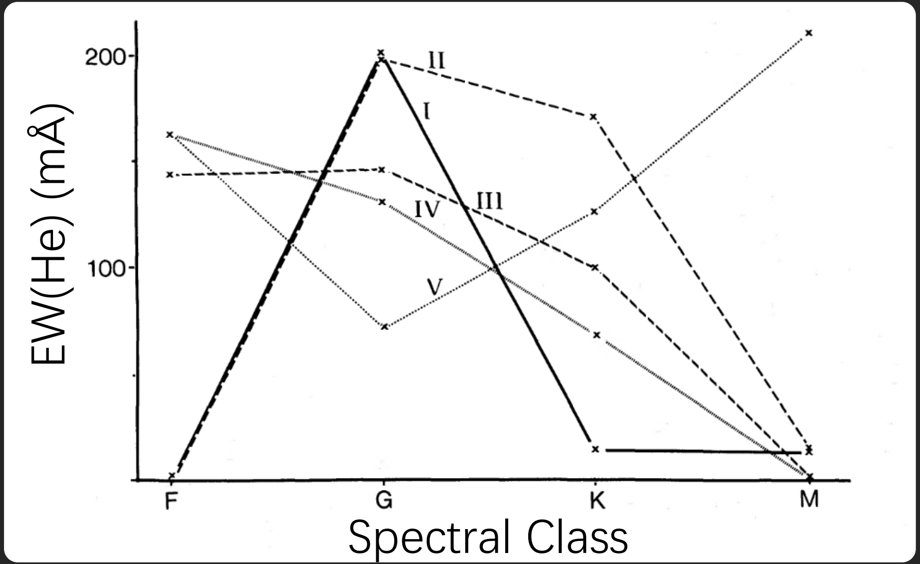

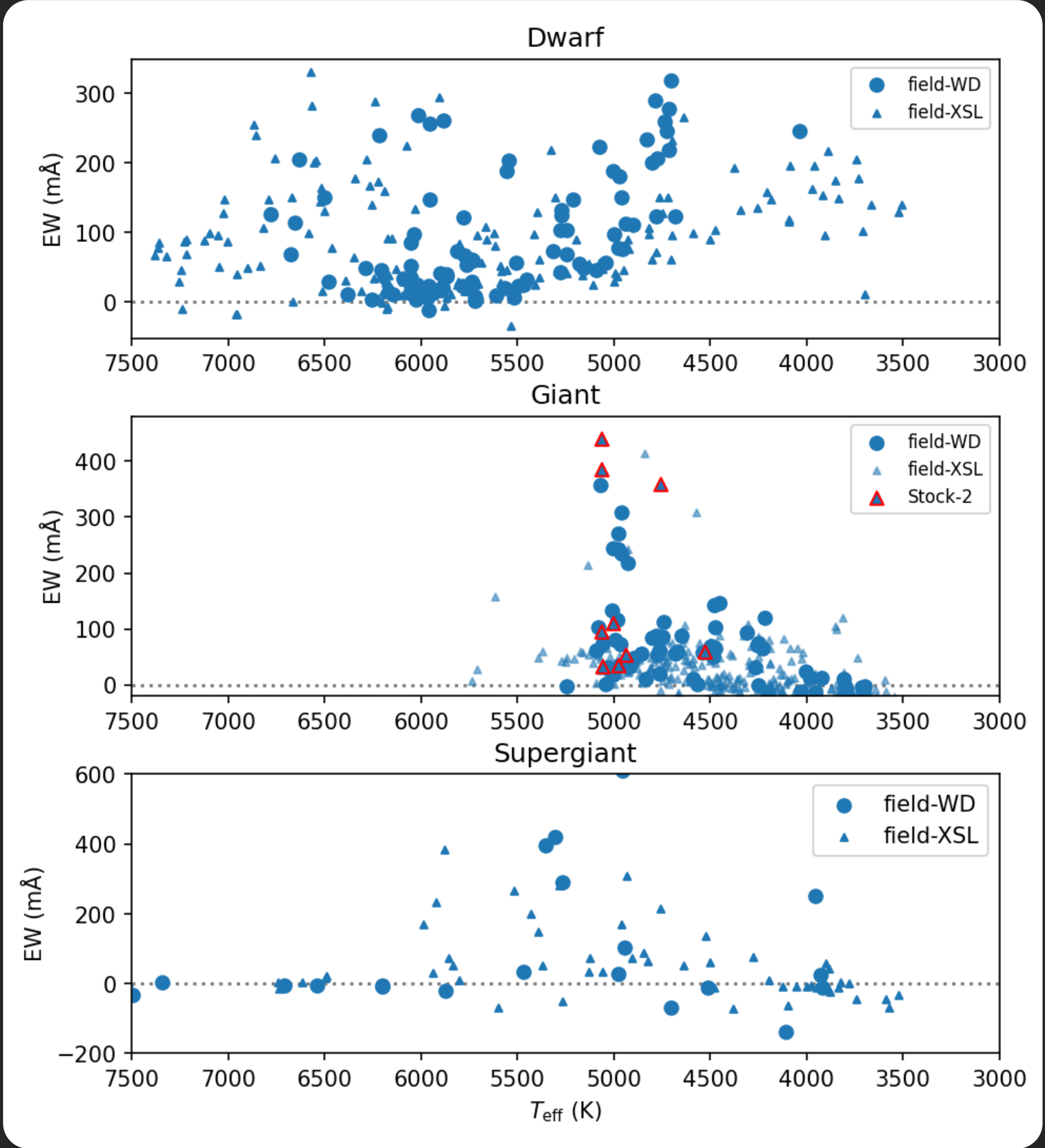

EW(He) - T_{eff} trend

- Dwarf
  - Main and secondary trend;
  - A clear lower boundary in the main trend;
  - Scatter above the lower boundary appears.
- Giant
  - The average EW is smaller than the dwarf's
  - Metal-poor stars tend to have smaller EW.

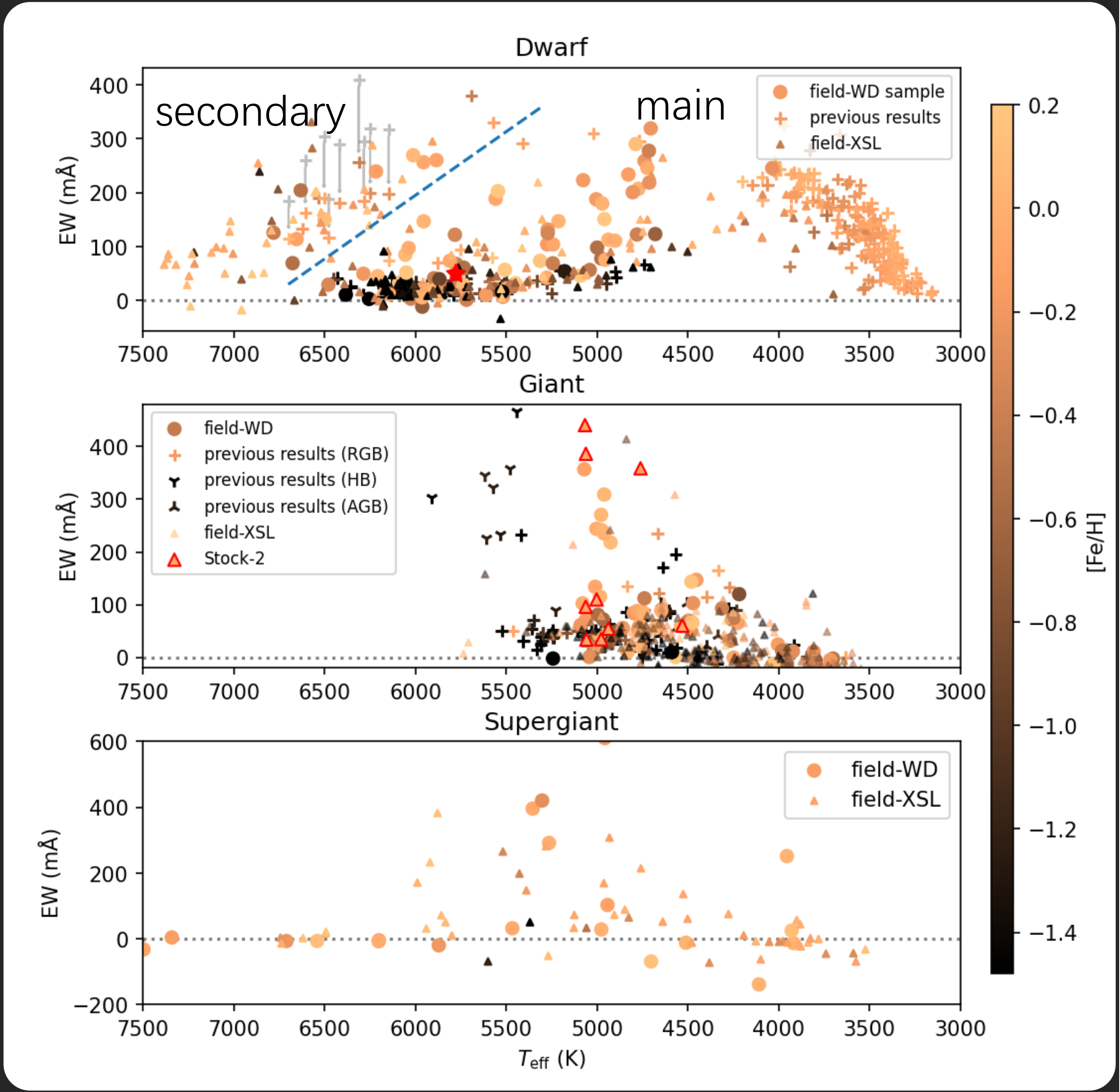

EW(He) - T_{eff} trend

- The increase of EW(He) is consistent with that in $\log R'_{\mathrm{HK}}$.
- Such behavior implies that the CE formation mechanism appears, in the dwarfs near the lower boundary.

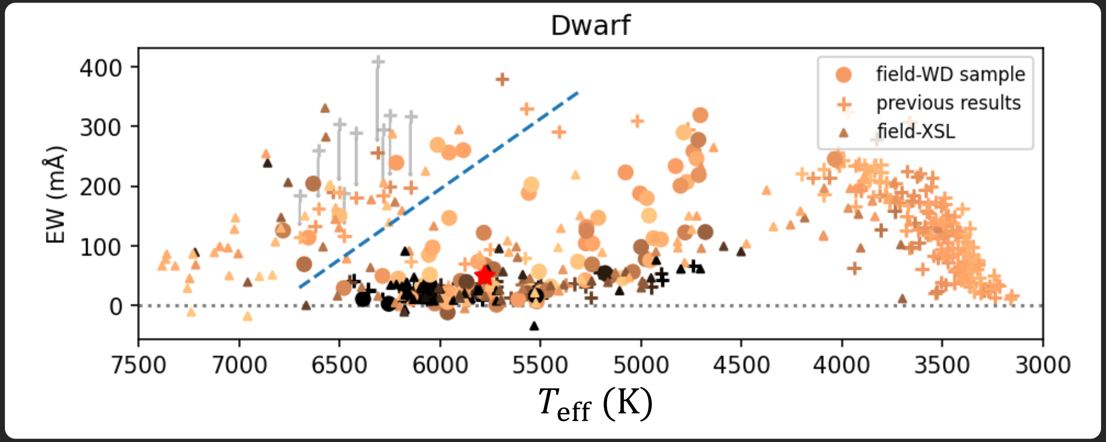

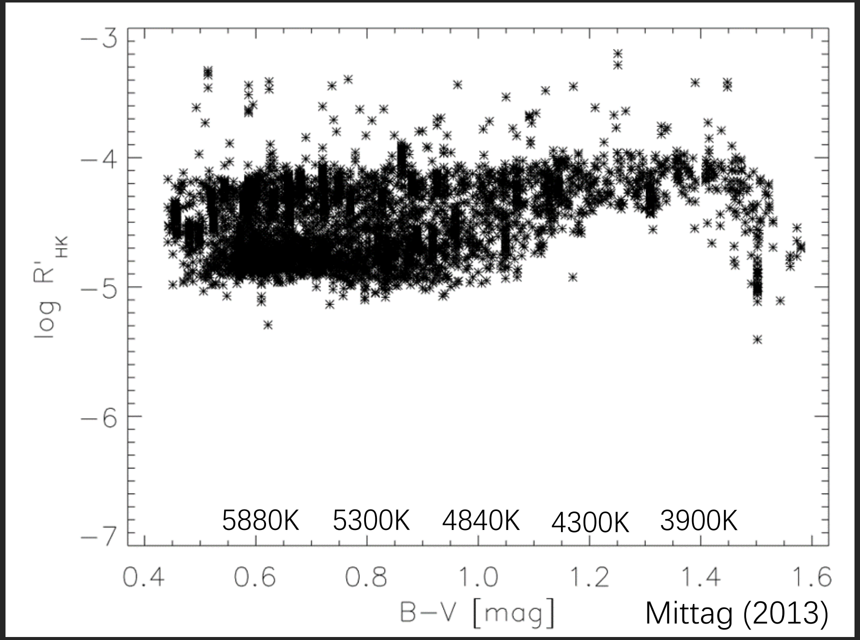

(Fig. 6.4)

EW(He) - T_{eff} trend

with $\log R'_{\mathrm{HK}}$

- $\log R'_{\mathrm{HK}}$ is larger at $T_{\mathrm{eff}}{\sim}4000$K, and smaller in lower/higher temperatures.
- $\log R'_{\mathrm{HK}}$ is also correlated with EW(He) in Stock-2 giants.

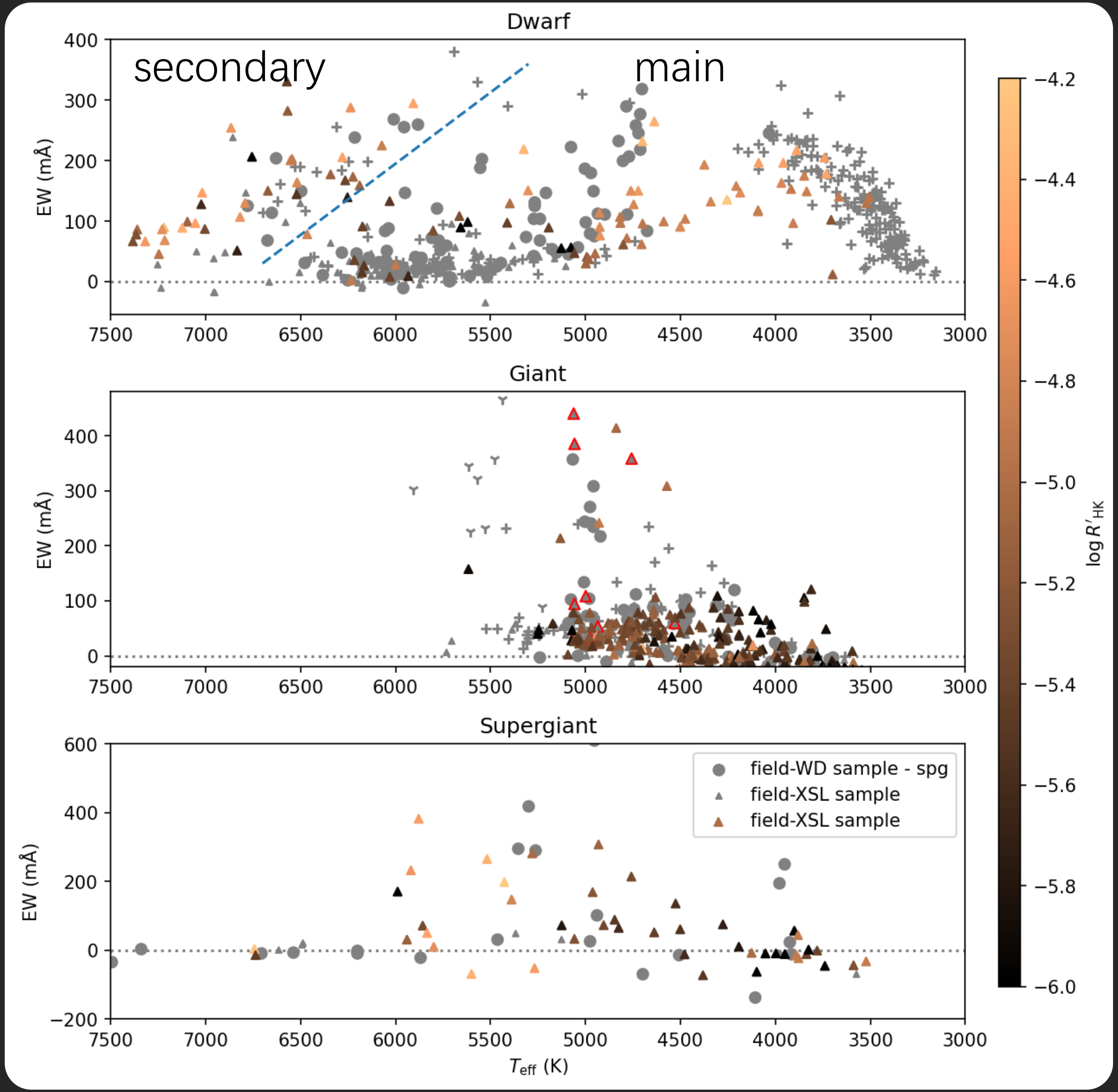

EW(He) - T_{eff} trend

with L_{X}

- The dwarfs with larger EW(He) also have stronger X-ray radiation.
- The He 10830 for the dwarfs above the lower boundary are dominated by the PR mechanism.
- Such trend is seen but not obvious in the warm giants.

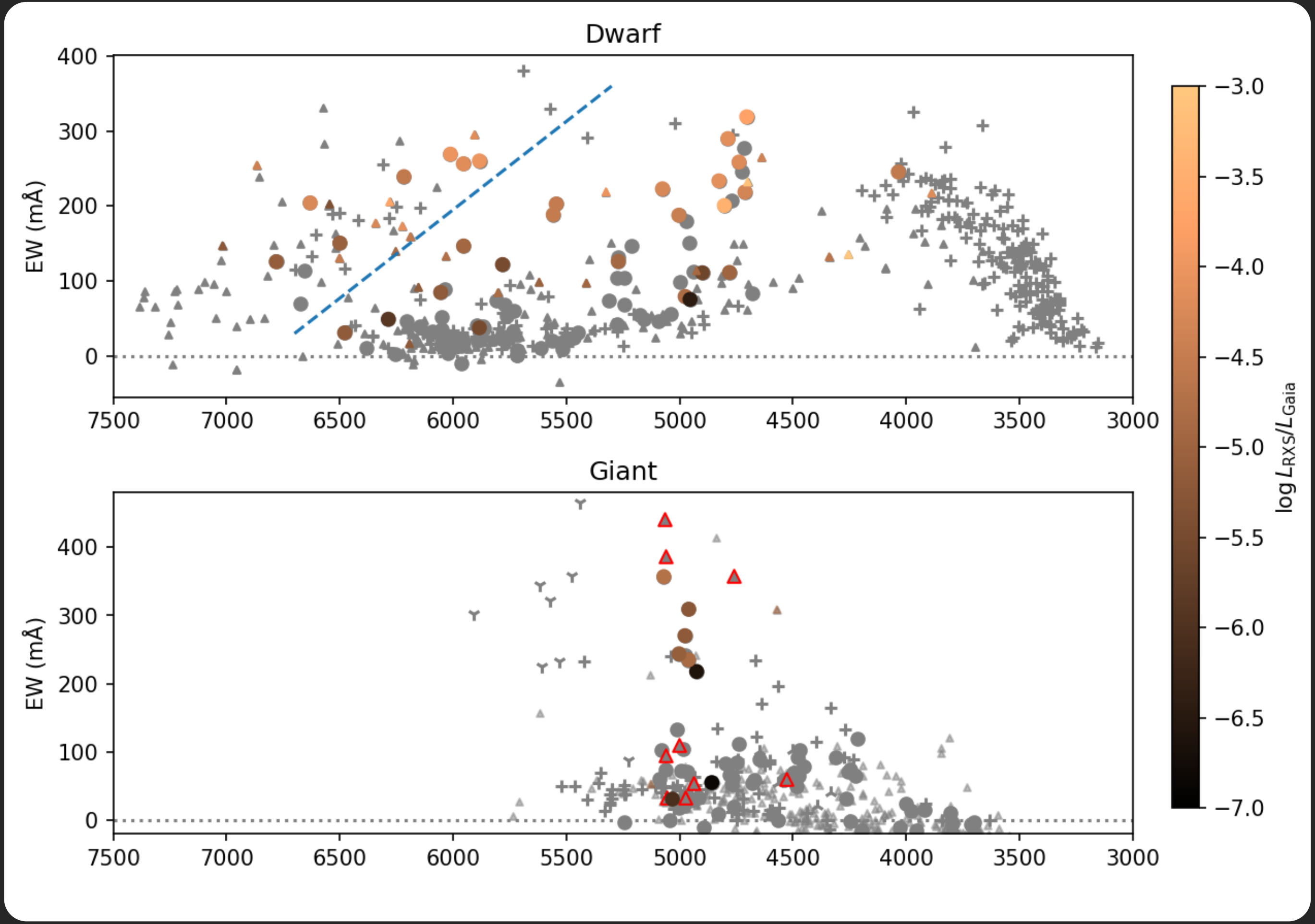

Summary

- The strength and shape of He 10830 and $\log R'_{\mathrm{HK}}$ for the red clump stars in Stock 2 are measured.
  - EW - $\log R'_{\mathrm{HK}}$ linear relation: larger than that for field stars
  - Symmetric line profile: stable chromospheres
- Some empirical trends between He 10830 EW and other parameters present for field stars.
- Observations in He and Ca II line for more cluster would further confirm the possibility of using He 10830 as a helium abundance indicator.

How to extend: 1. More stars

- More stars in blue:
  - SPA spectra for giants in other OCs.

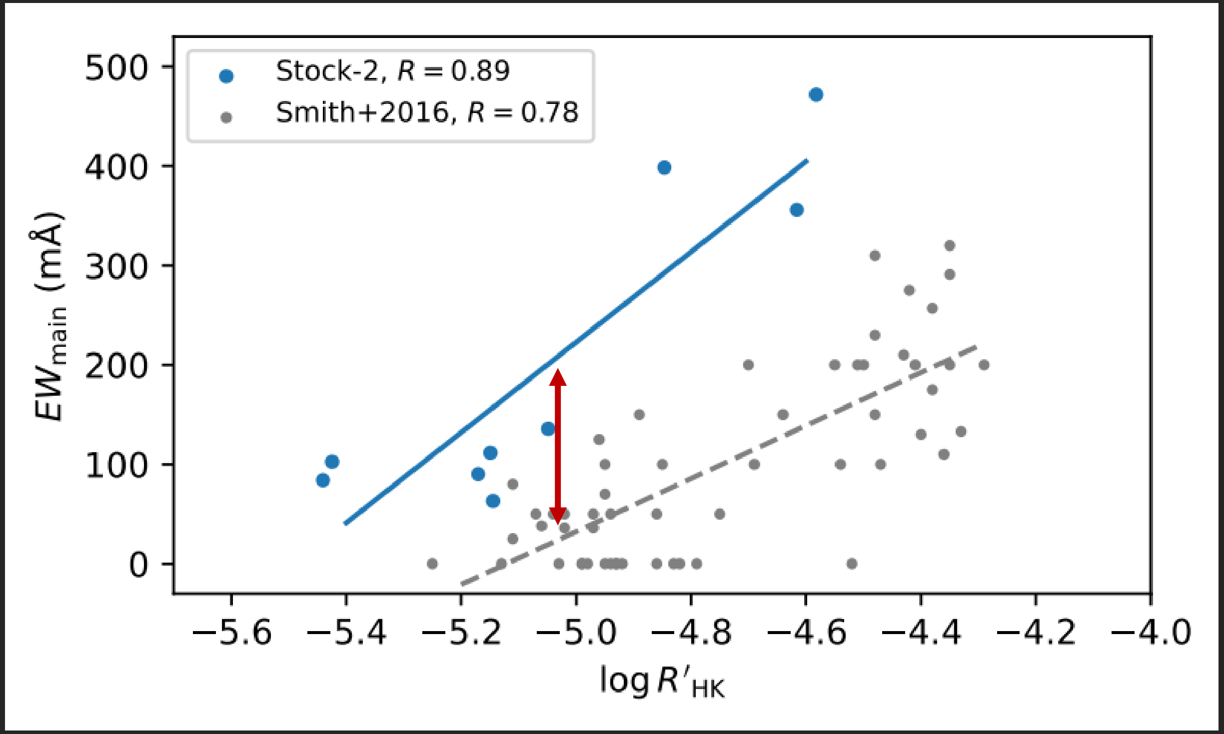

How to extend: 2. Globular cluster?

- P110: 110.2446 (PI: Jian)
- X-Shooter for NGC2808 stars

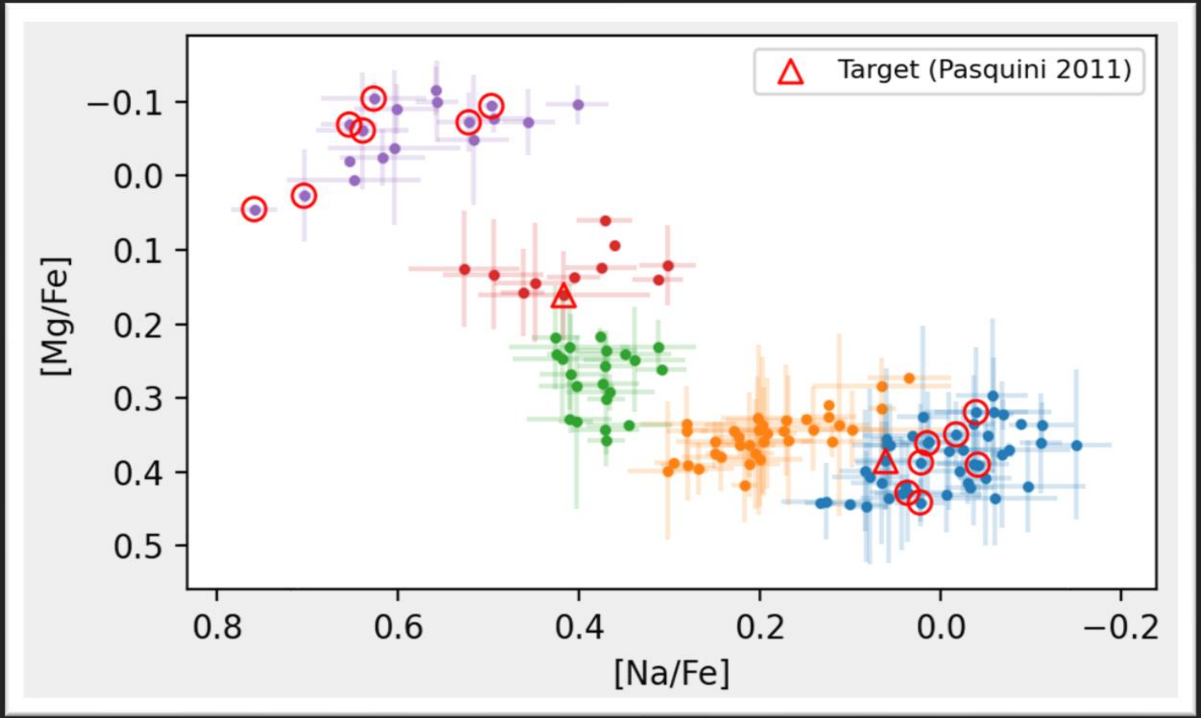

How to extend: 2. Globular cluster?

- The

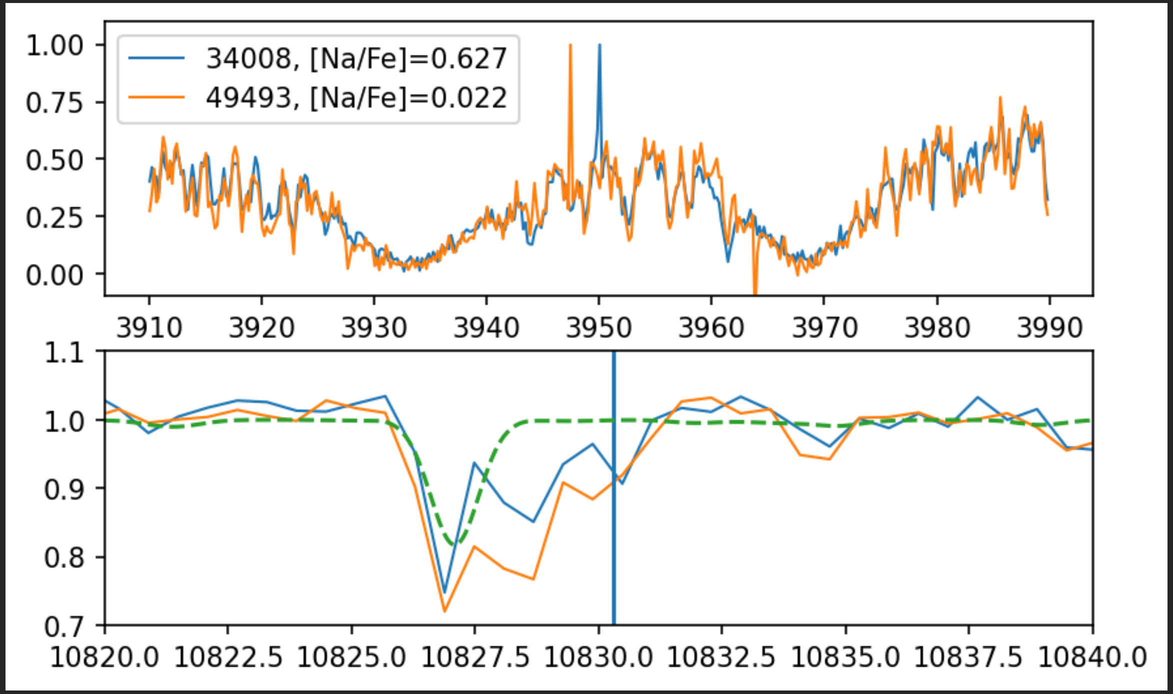

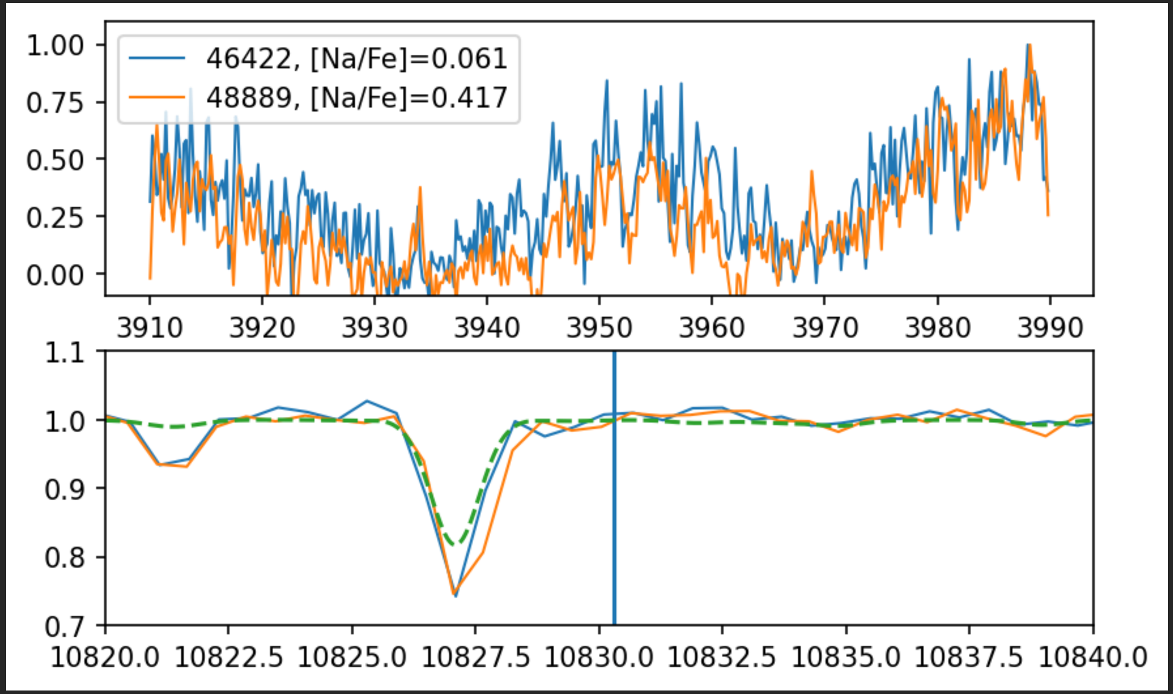

Previous observations

Can previous observations tell us about the information of PR/CE mechanism?

(Chapter 2 in the thesis)

Targets and measurements

What new targets are available? (Chapters 3-5 in the thesis)

EW(He), $\log R'_{\mathrm{HK}}$ and L_{X} measurement

- $N_{\mathrm{all}} = 749$
- EW(He): 719
- $\log R'_{\mathrm{HK}}$: 392
- $\log L_{\mathrm{X}}/L_{\mathrm{Gaia}}$: 72
  - XMM-Newton
  - ROSAT
- A large sample of EW(He) measurement is derived.

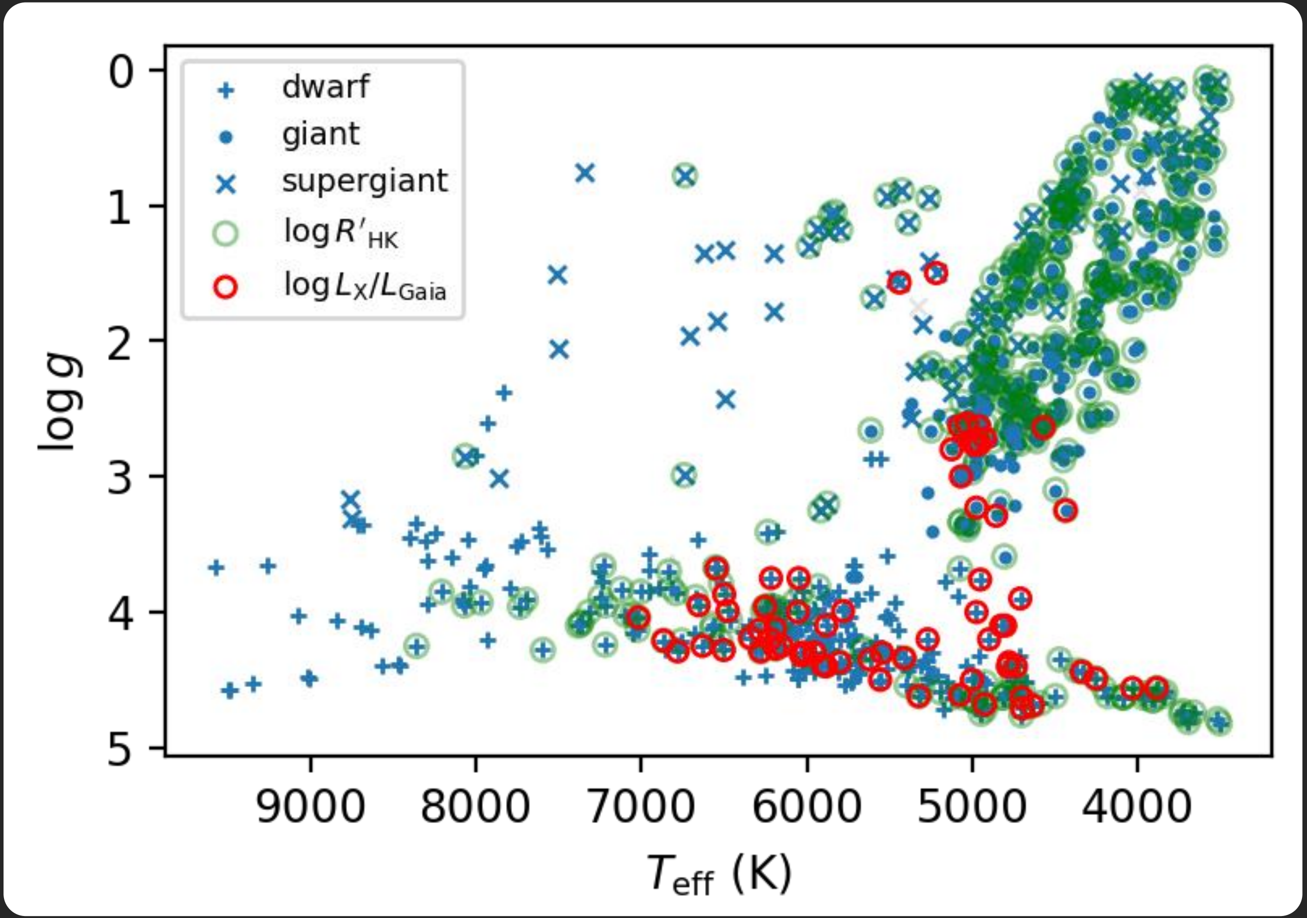

Discussion

Can He 10830 be used to determine Y, and if so, which star should be the target? (Chapter 8 in the thesis)

EW(He)-[Fe/H] relation
in cool giants

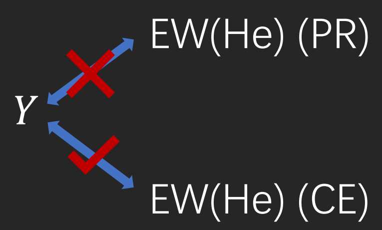

- Giants rightward of the dividing line would be CE dominated.

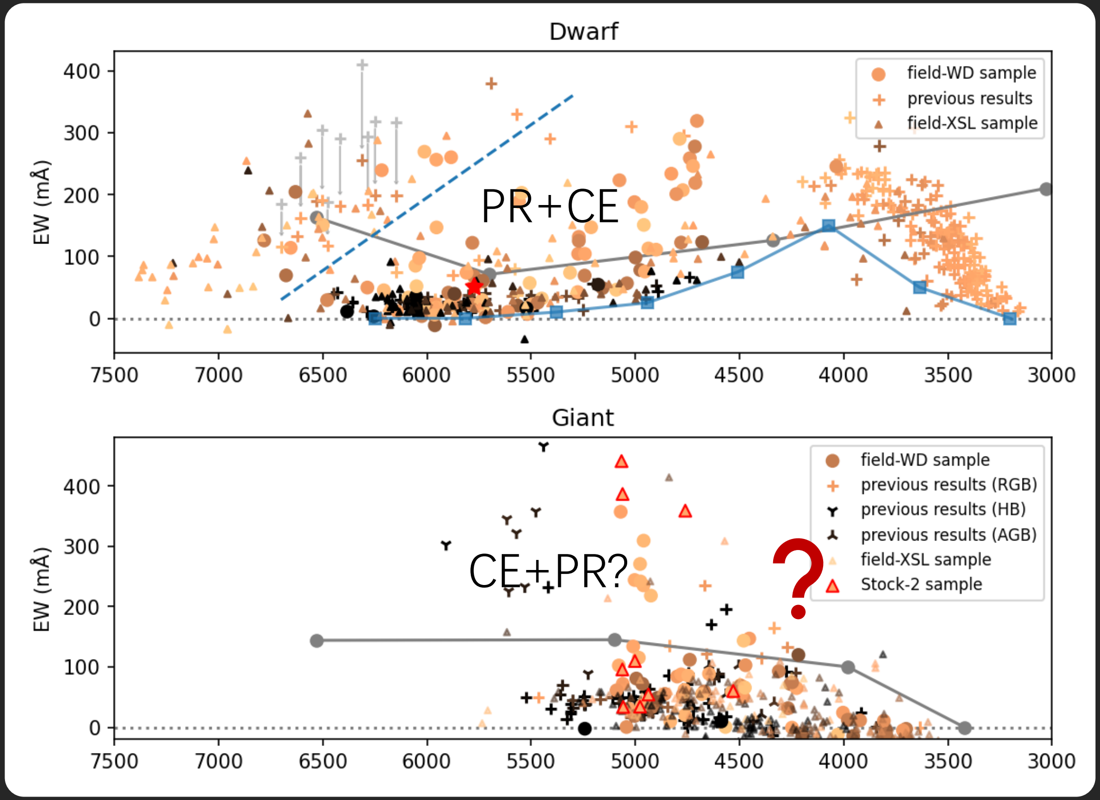

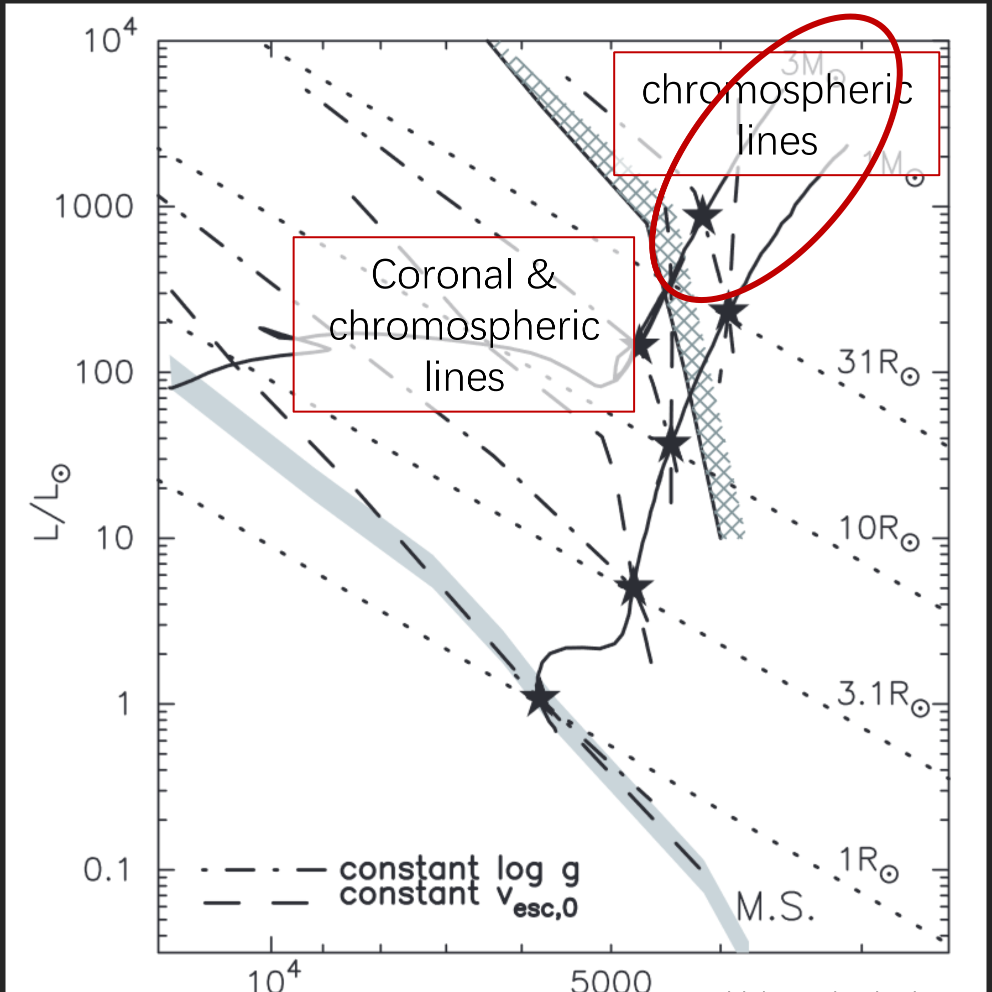

Suzuki (2007), Linsky & Haish (1979)

EW(He) – [Fe/H] relation
for cool giants

(Fig. 8.3)

- Positive relations between EW(He) and [Fe/H] are found in field-XSL giants with $4300 < T_{\rm eff} < 4700{\rm K}$.
- If they are dominated by CE mechanism, then such relation would be caused by Y variation.

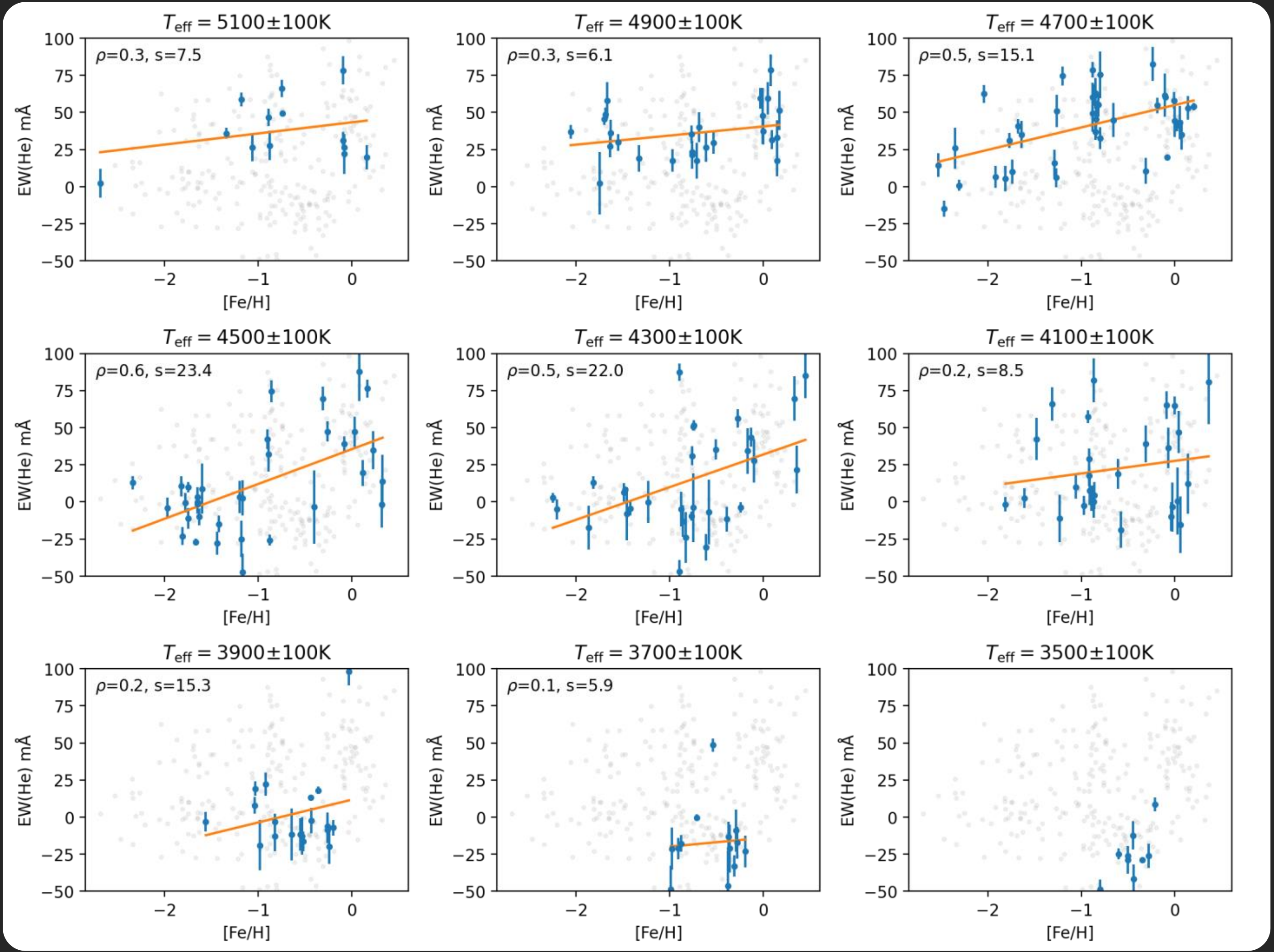

Connection between He 10830 and Y
in globular cluster (GC) members

- *"If spectra could be obtained in a globular cluster, providing a larger sample of similar stars, the relative abundance of helium might be assessed."*

  -- Dupree+ (2009)

- The evidence of He 10830 equivalent width (EW) difference is not obvious.

(Fig. 1.4)

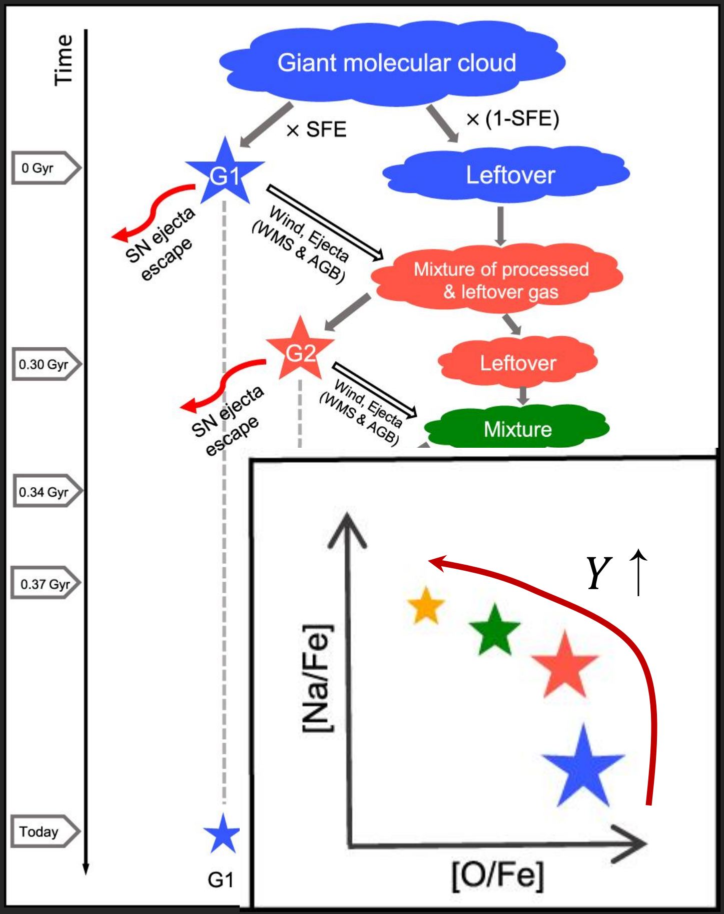

Kim&Lee (2018)

(Fig. 8.1)

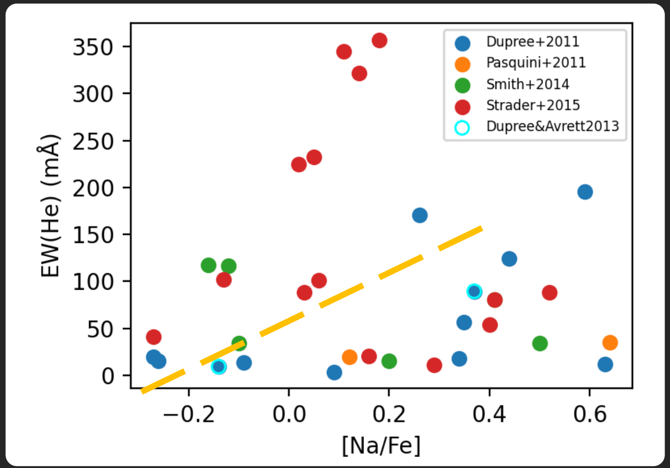

Study	GC	Number of stars
Smith et al. (2014)	M13	6
Pasquini et al. (2011)	NGC2808	2
Dupree & Avrett (2013)	ω Cen	2
Smith et al. (2014)	M13	6
Navarrete et al. (2015)	ω Cen	24
Strader et al. (2015)	M4	16

Previous selections of targets in GCs

- Most of the targets are hotter than $4500\mathrm{K}$, which is expected to have some extent of corona.
- Future observation aiming to probe Y difference should focus on the giants with $T_{\mathrm{eff}} < 4500\mathrm{K}$.

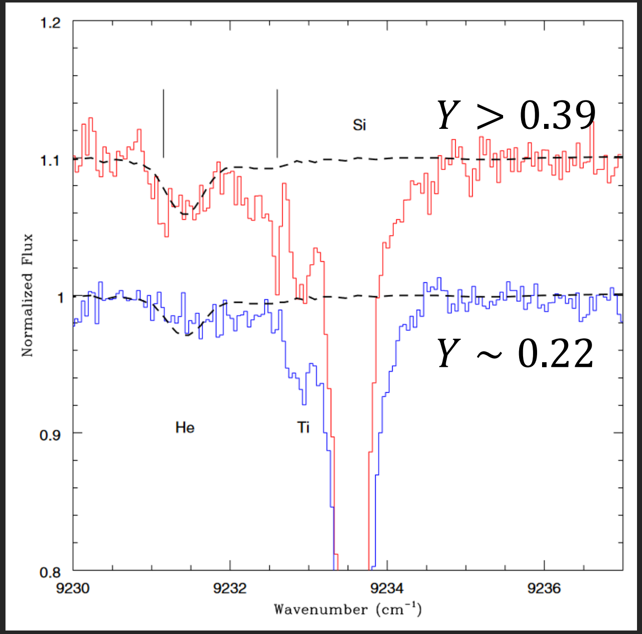

Pasquini (2011)

(Fig. 8.1)

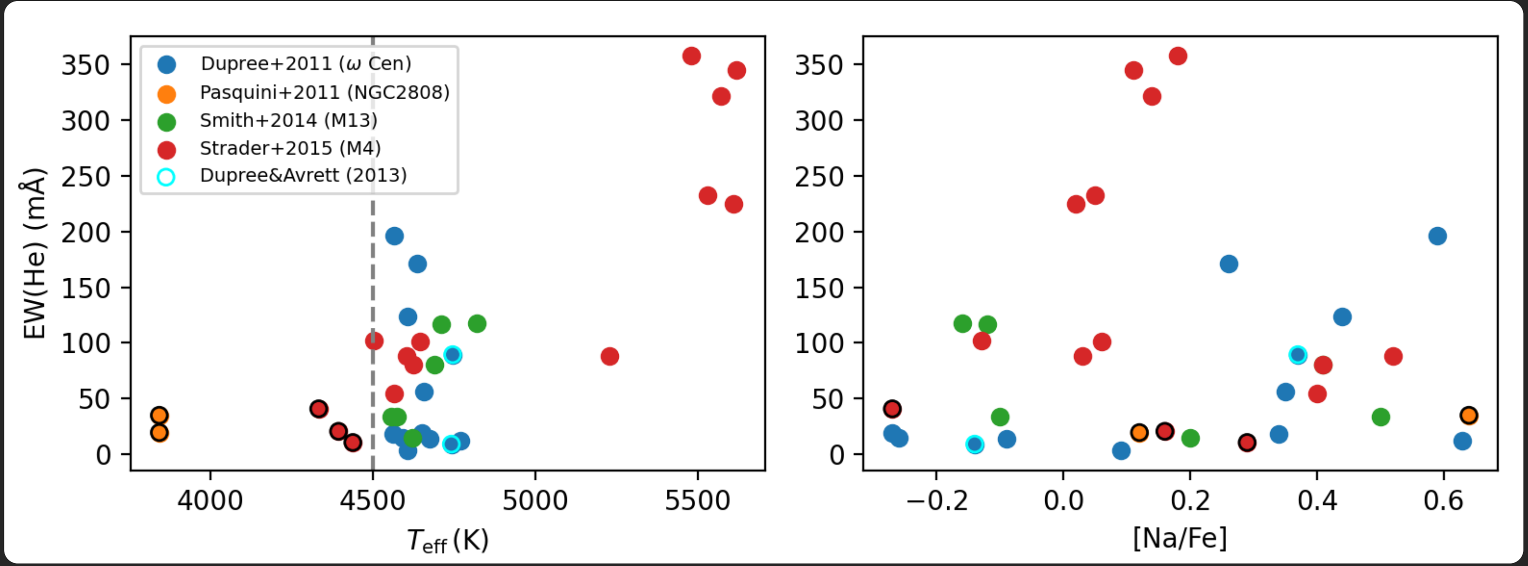

Table of contents

Introduction

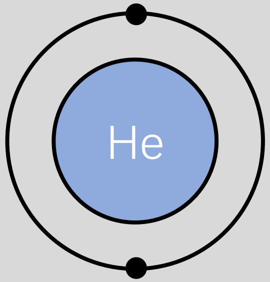

Synthesis

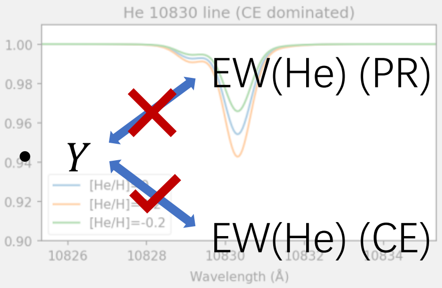

- Y
  - EW(He) (PR)
  - EW(He) (CE)

Previous observation

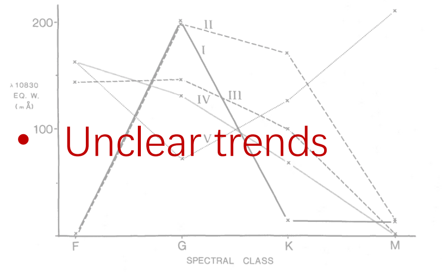

- Unclear trends

Targets and measurements

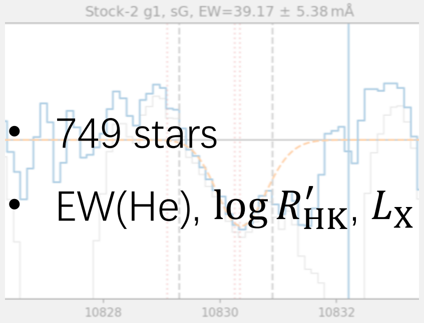

- 749 stars
- EW(He), $\log R'_{\mathrm{HK}}$, L_{X}

Empirical trends

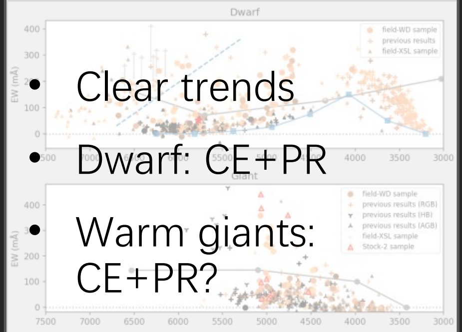

- Clear trends
- Dwarf: CE+PR
- Warm giants: CE+PR?

Discussion

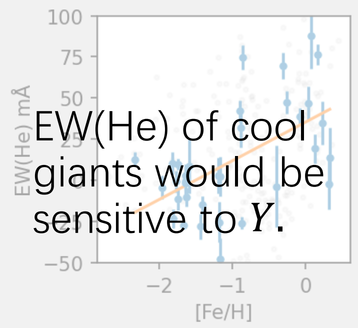

- EW(He) of cool giants would be sensitive to Y.

Conclusion

- What we know about the He 10830:

	Before	After
$\mathrm{EW(He)}$-T_{eff} trend	Rough trends	Detail trends from ~750 stars.
PR/CE mechanism	Exist in dwarfs and giants	Switch between PR/CE for dwarfs and giants
Y sensitivity	---	Only in CE dominated lines
GC target selection	Warm giants (stronger He 10830)	Cool giants (avoid PR mechanism)

Future perspective

- One step closer to the Y from He 10830:
- EW(He) for cool stars are sensitive to Y.

cool giants

- Reveal the relative Y difference for ~~stars~~ with similar stellar parameters.
  - Globular cluster members.
  - Bulge stars.
- Measure Y using He 10830 and detailed chromospheric modelling.
  - (though the method needs to be established yet)

Planned observations

- M5: UT22-2-013 with HPF@McDonald;
- NGC2808: 0110.D-4258(A) with X-Shooter@VLT.
- We expect the EW of He 10830 will be different for the stars in different stellar populations.

M5 $(T_{\text{eff}} < 4500\text{K})$ NGC2808

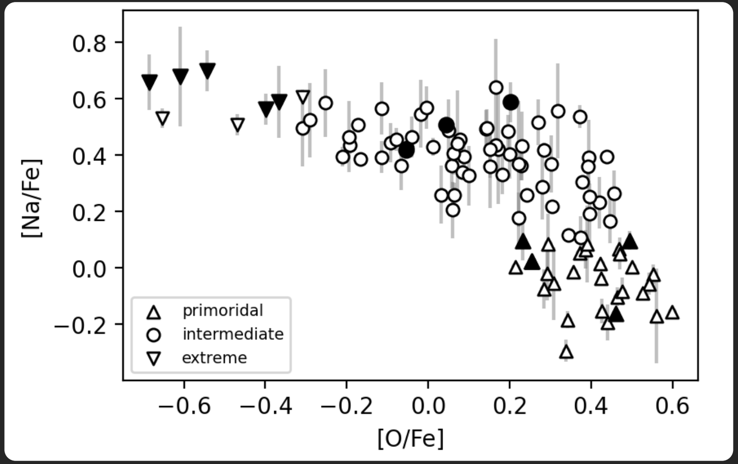

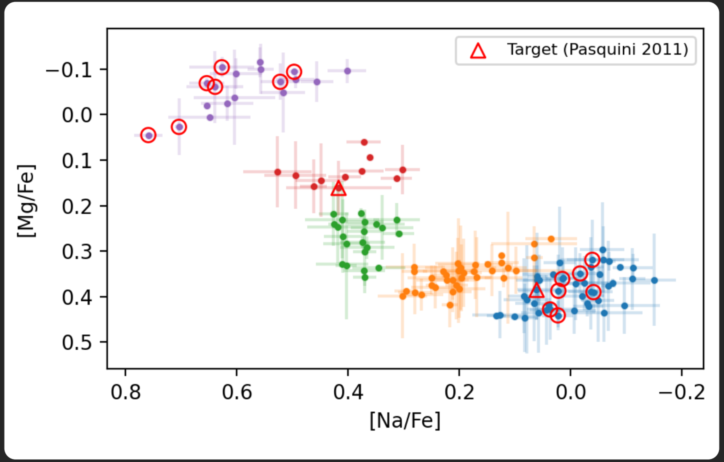

- [Fe/H]: -2~0.2

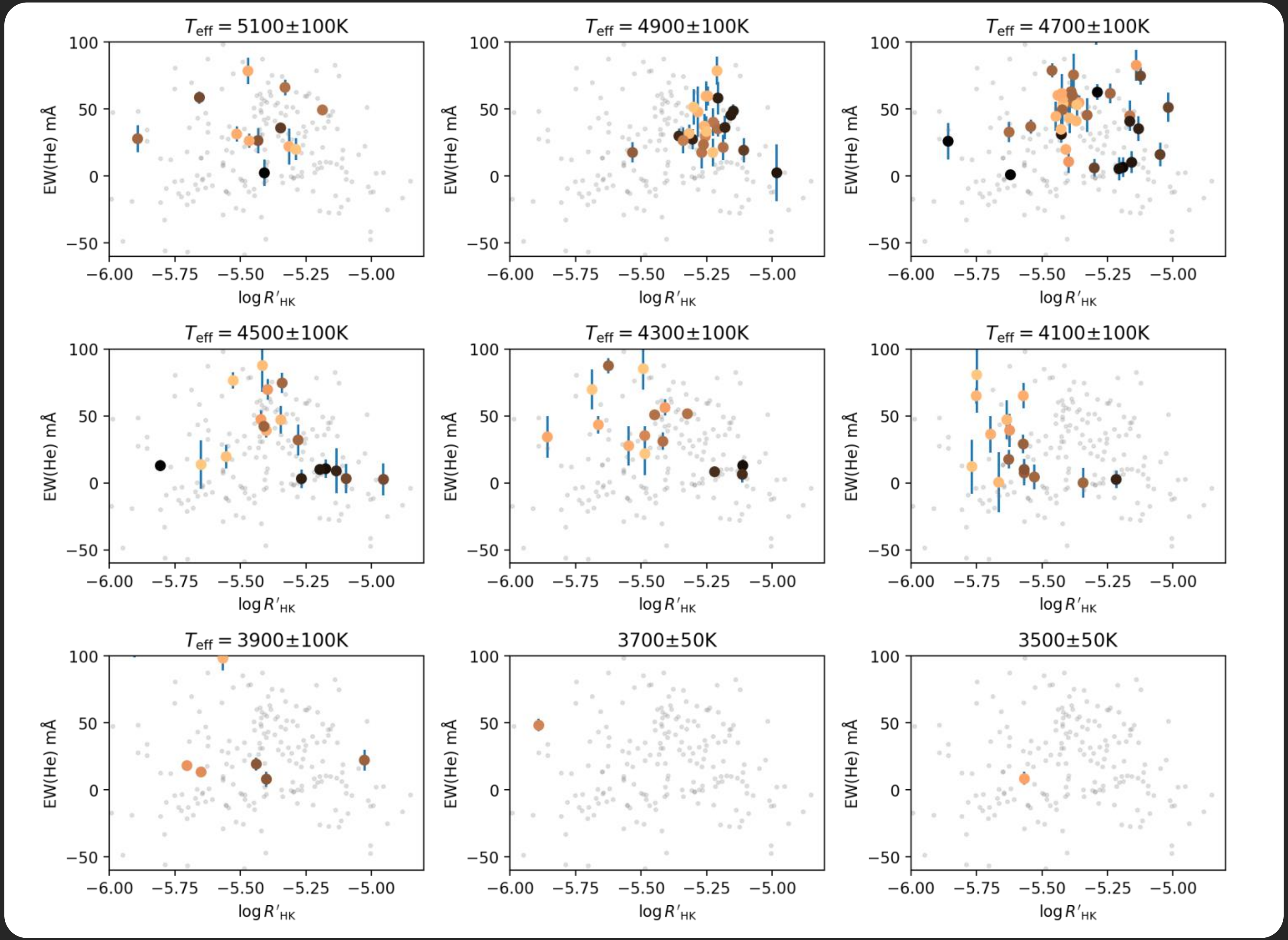

T_{eff} = 5100±100K
T_{eff} = 4900±100K
T_{eff} = 4700±100K
T_{eff} = 4500±100K
T_{eff} = 4300±100K
T_{eff} = 4100±100K
T_{eff} = 3900±100K
3700±50K
3500±50K
EW(He) mÅ
log R'_{HK}

FWHM-T_{eff} for field-WD stars

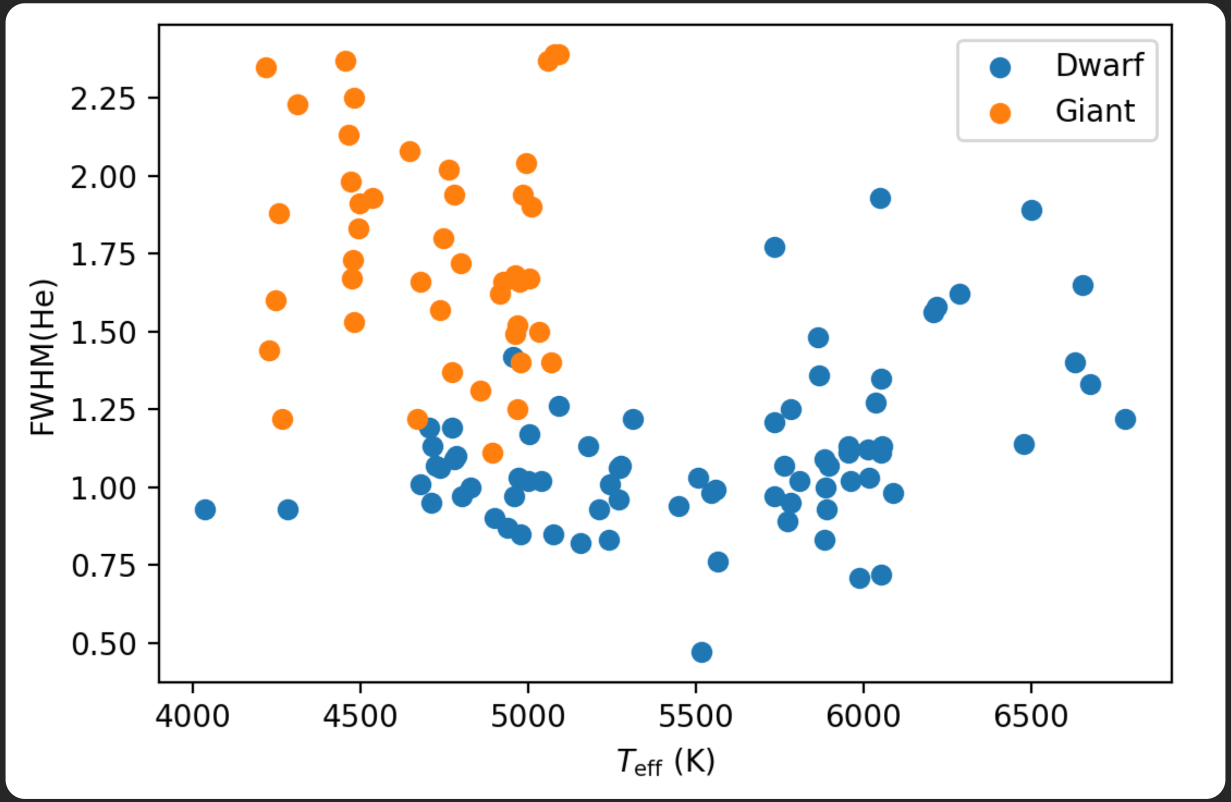

Synthesis of the He 10830

How does Y affect the feature? (Chapter 7 in the thesis)

NLTE radiative transfer calculation

for He 10830

- PR and CE; in chromosphere → NLTE
- Atmosphere model + atom model + external radiation:
  - → $\{n_\mathrm{H}\}$, Hα, Hβ lines;
  - → $\{n_\mathrm{He}\}$, He 10830;
  - → $\{n_\mathrm{CaII}\}$, Ca II H&K lines.
- External radiation: I
  - Tobiska (1991): $I_\mathrm{T}(\lambda)$ from 18 to 911Å;
  - Controls the amount of high-energy radiation.

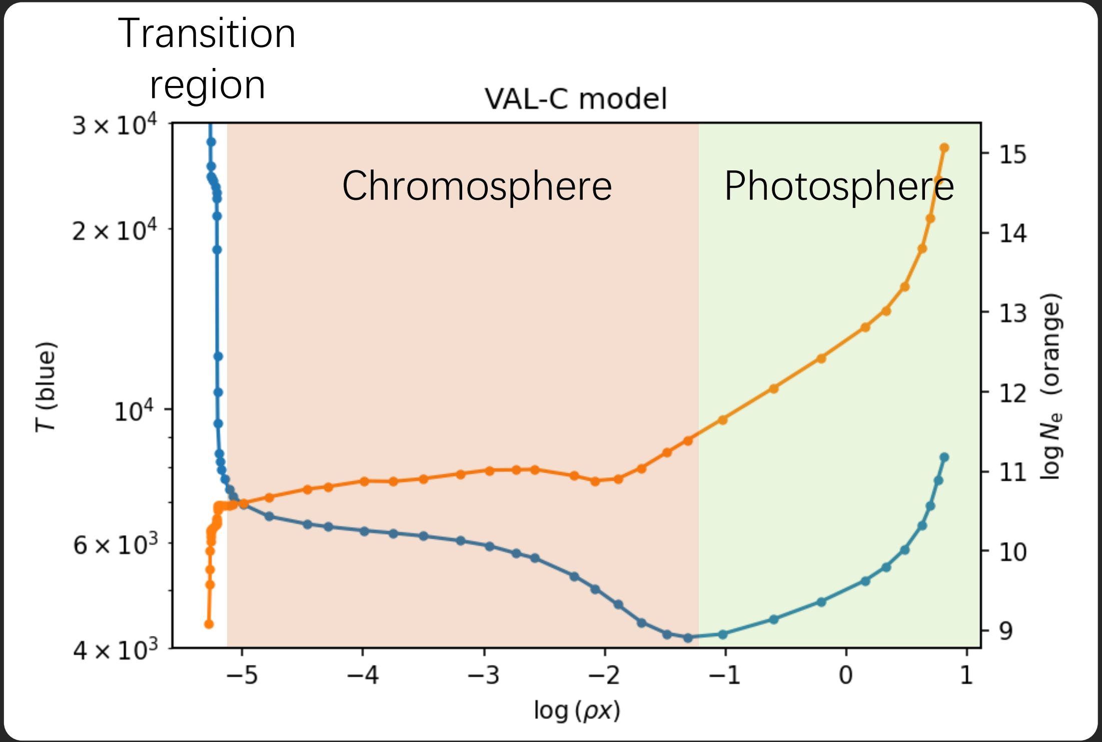

(Fig. 7.1)

outer, low-density ↔ inner high-density

PR dominated He 10830

- VAL-C model
- $I = 0, 10, 20, 30\ I_{\mathrm{T}}$
- H and Ca II lines are not affected by external radiation, while He 10830 is sensitive to I.

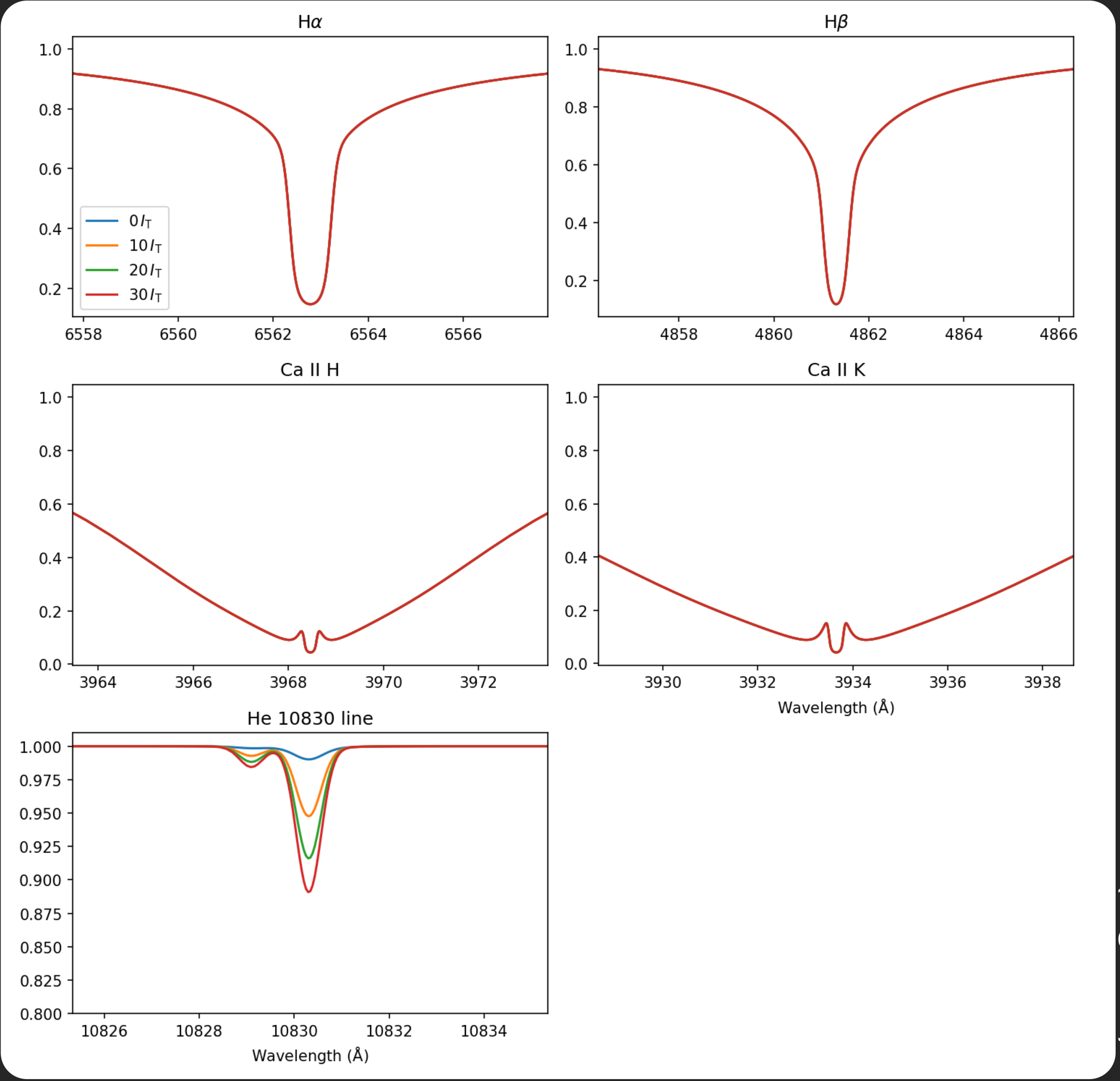

(Fig. 7.7)

CE dominated He 10830

- $I = 0$.
- Varying the position of temperature rise ⇔ changing chromospheric density.
- EW(He) is sensitive to chromospheric density, so does the Ca II line core emission ($\log R'_{\mathrm{HK}}$ increases).

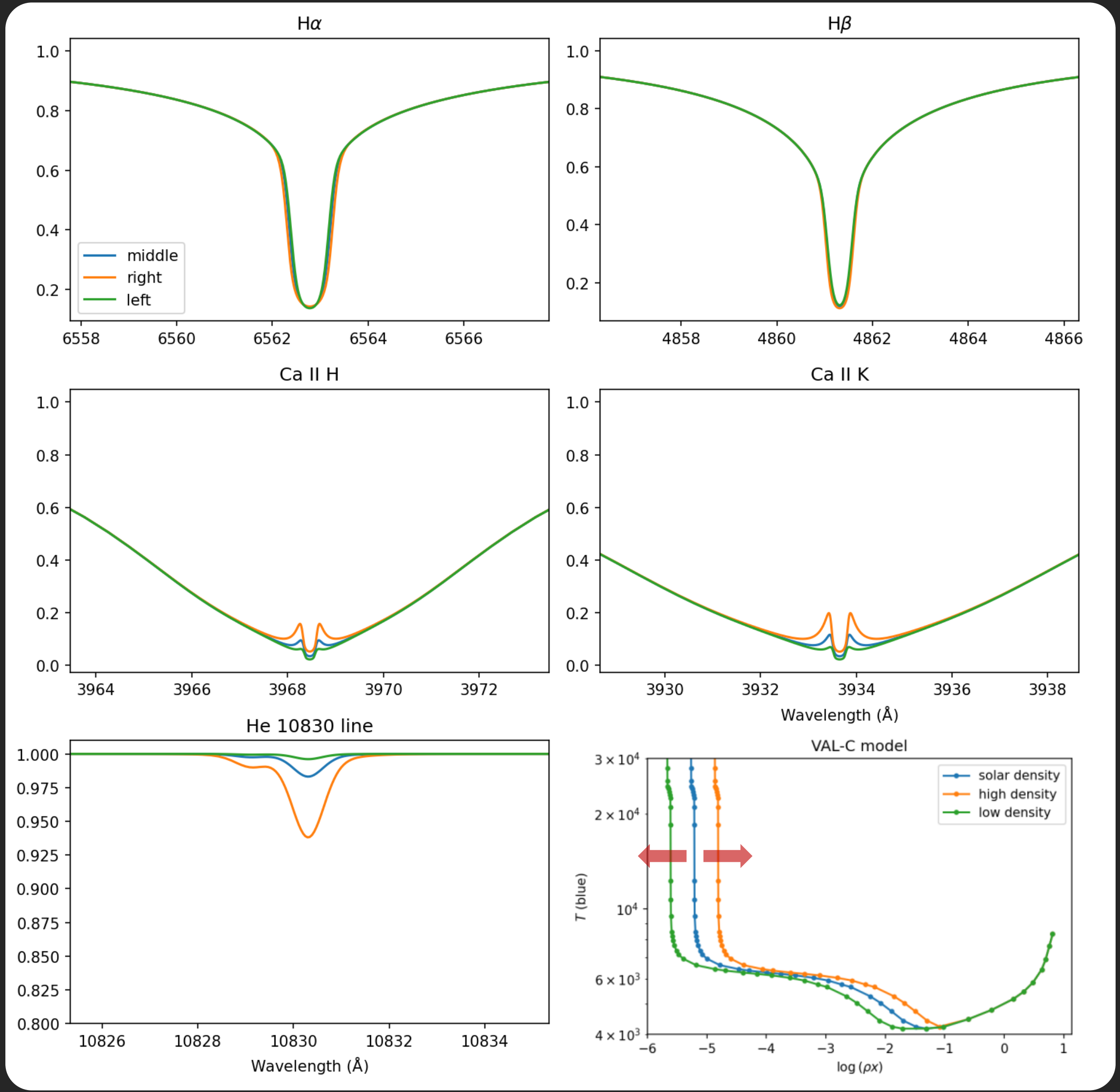

(Fig. 7.11, 7.12)

Sensitivity of the EW to Y

- PR dominated He 10830 only have a small sensitivity to helium abundance.
- CE dominated He 10830 is sensitive to helium abundance.

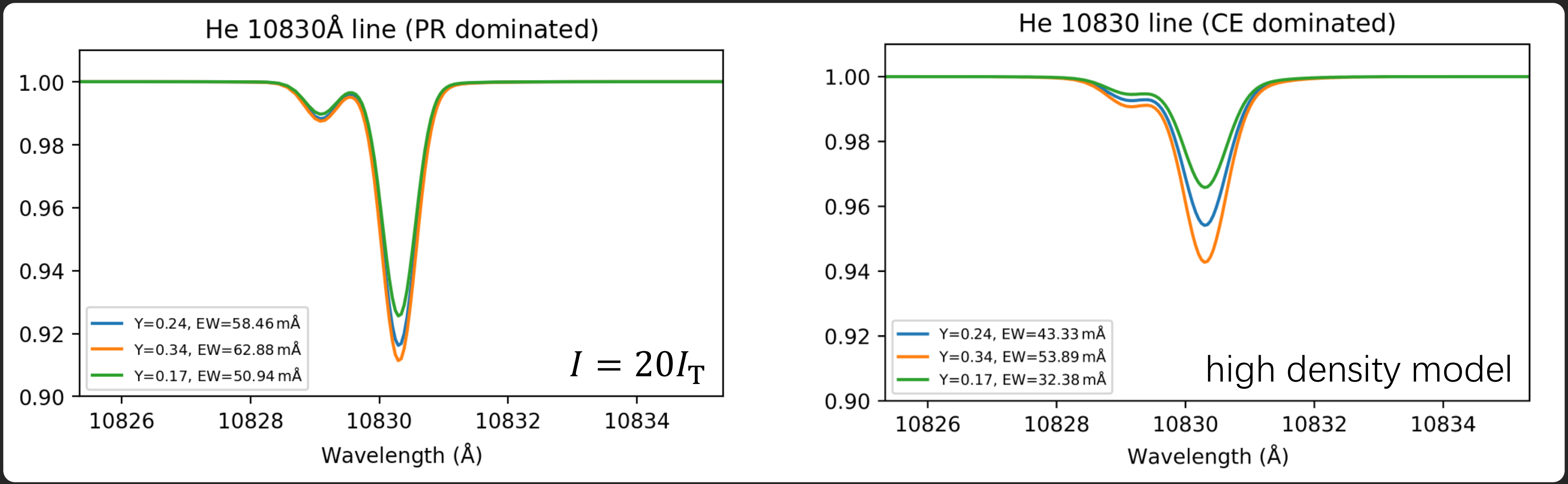

(Fig. 7.14, 7.15)

Explaining the sensitivity

Using the $2^3S(1s2s)$ populations in PR/CE

PR dominant case

- I absorbed by He I
- $\mathrm{EW(He)} \propto I$

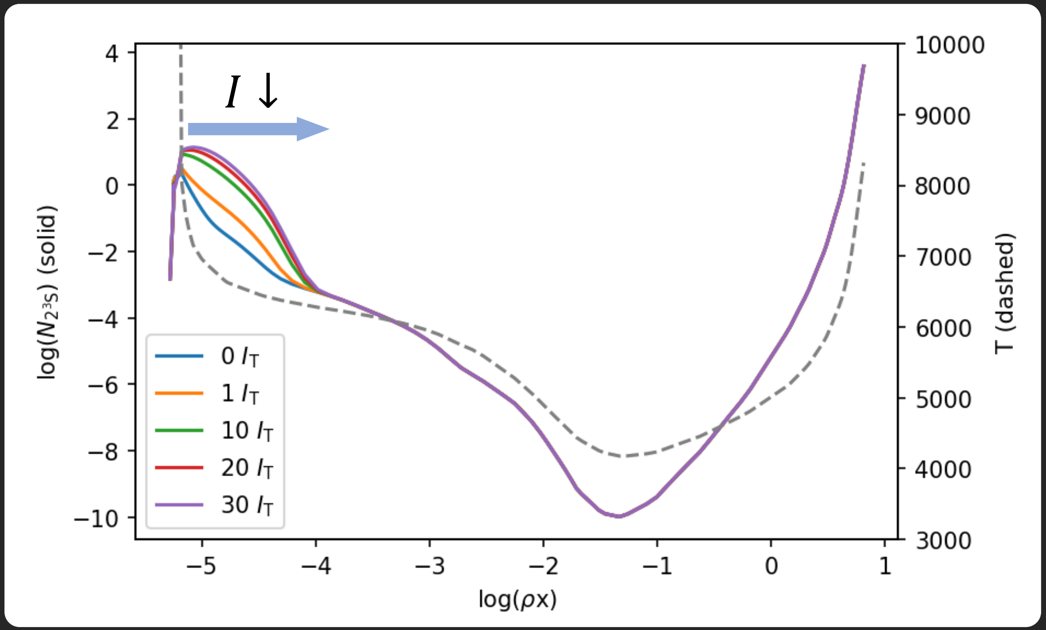

(Fig. 7.10)

CE dominant case

- CE rate $\propto n_e, n_{1s^2}$
- $\mathrm{EW(He)} \propto Y$

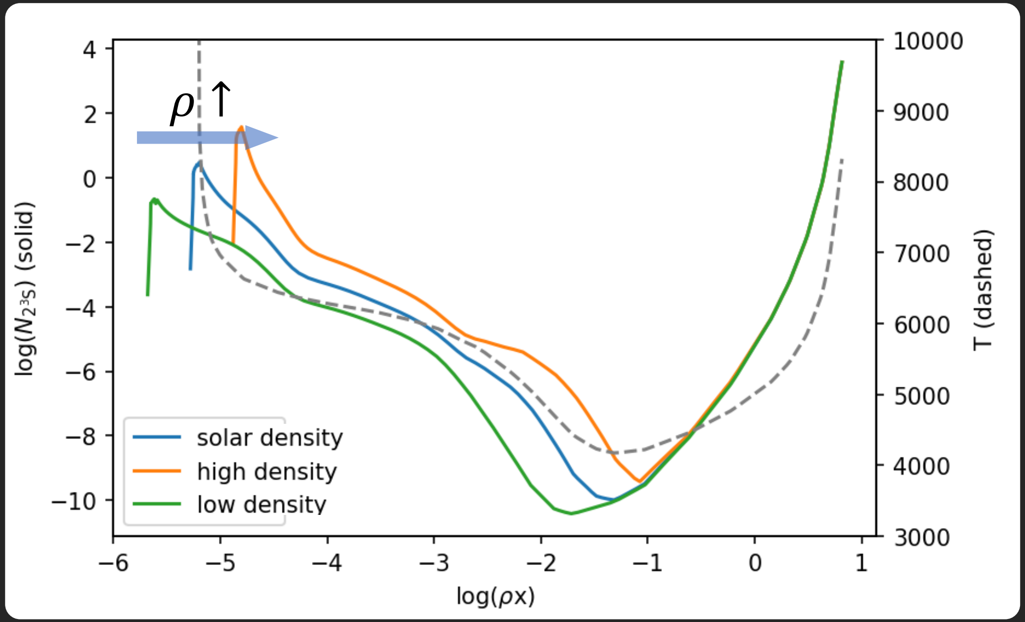

Table of contents

Introduction

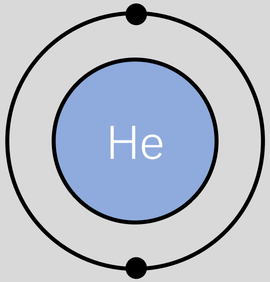

Synthesis

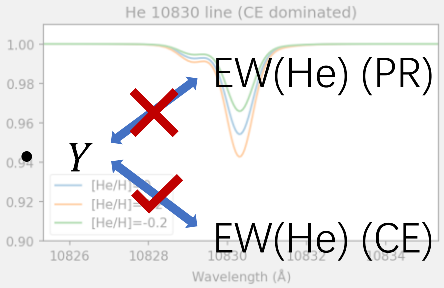

Previous observation

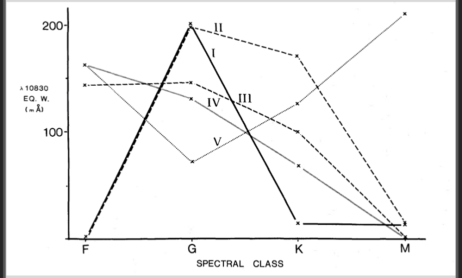

Targets and measurements

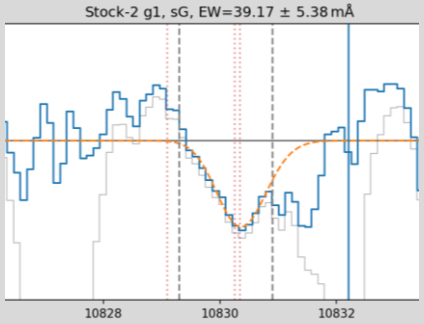

Empirical trends

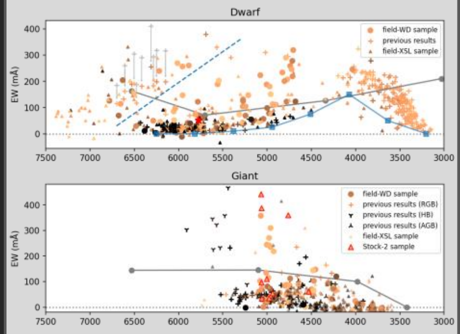

Discussion

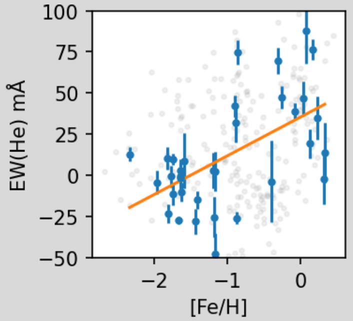

Fig 1.7

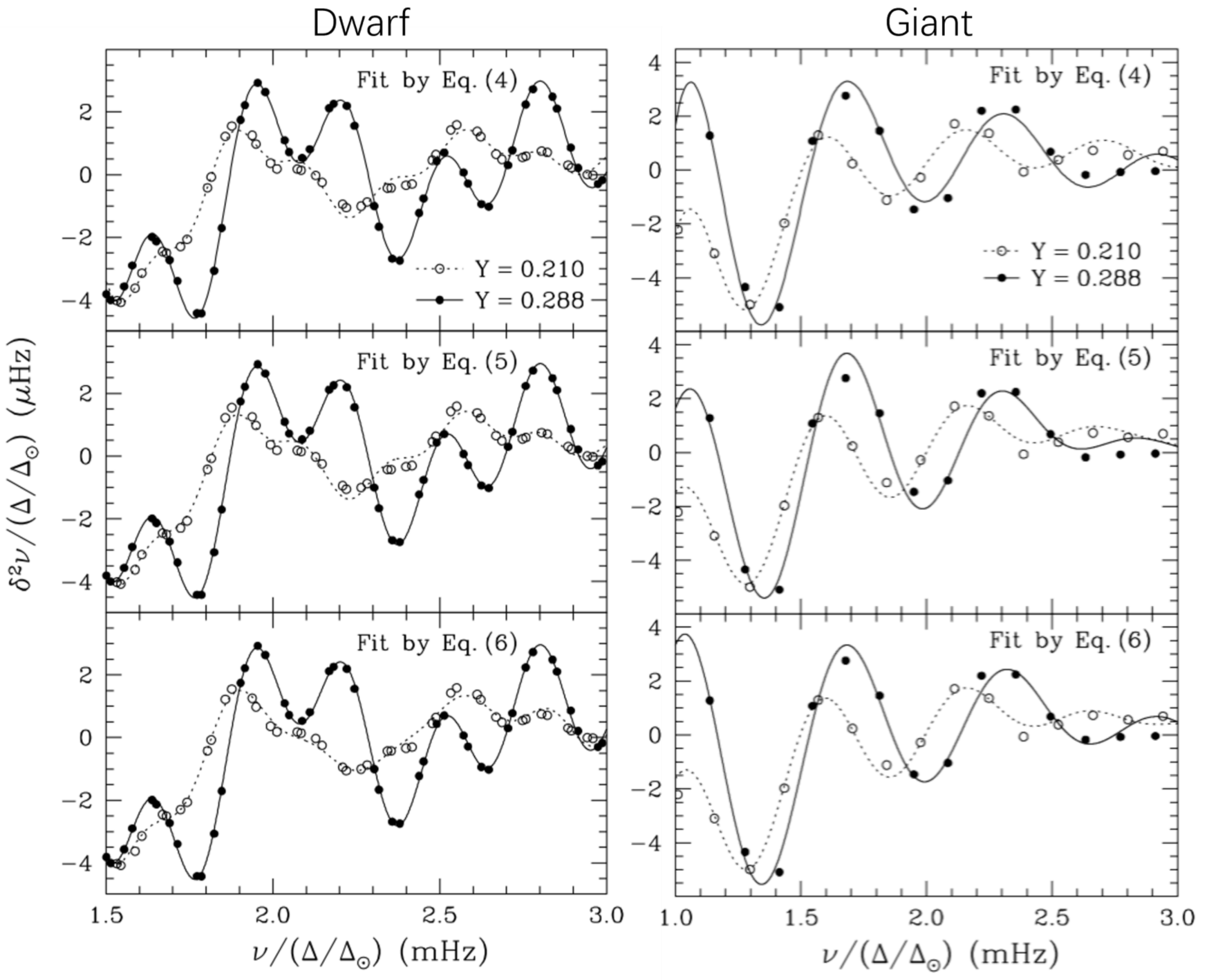

Dwarf
Giant
Fit by Eq. (4)
Fit by Eq. (5)
Fit by Eq. (6)
Y = 0.210
Y = 0.288
$\delta^2\nu/(\Delta/\Delta_\odot)$ (μHz)
$\nu/(\Delta/\Delta_\odot)$ (mHz)

Fig 1.8

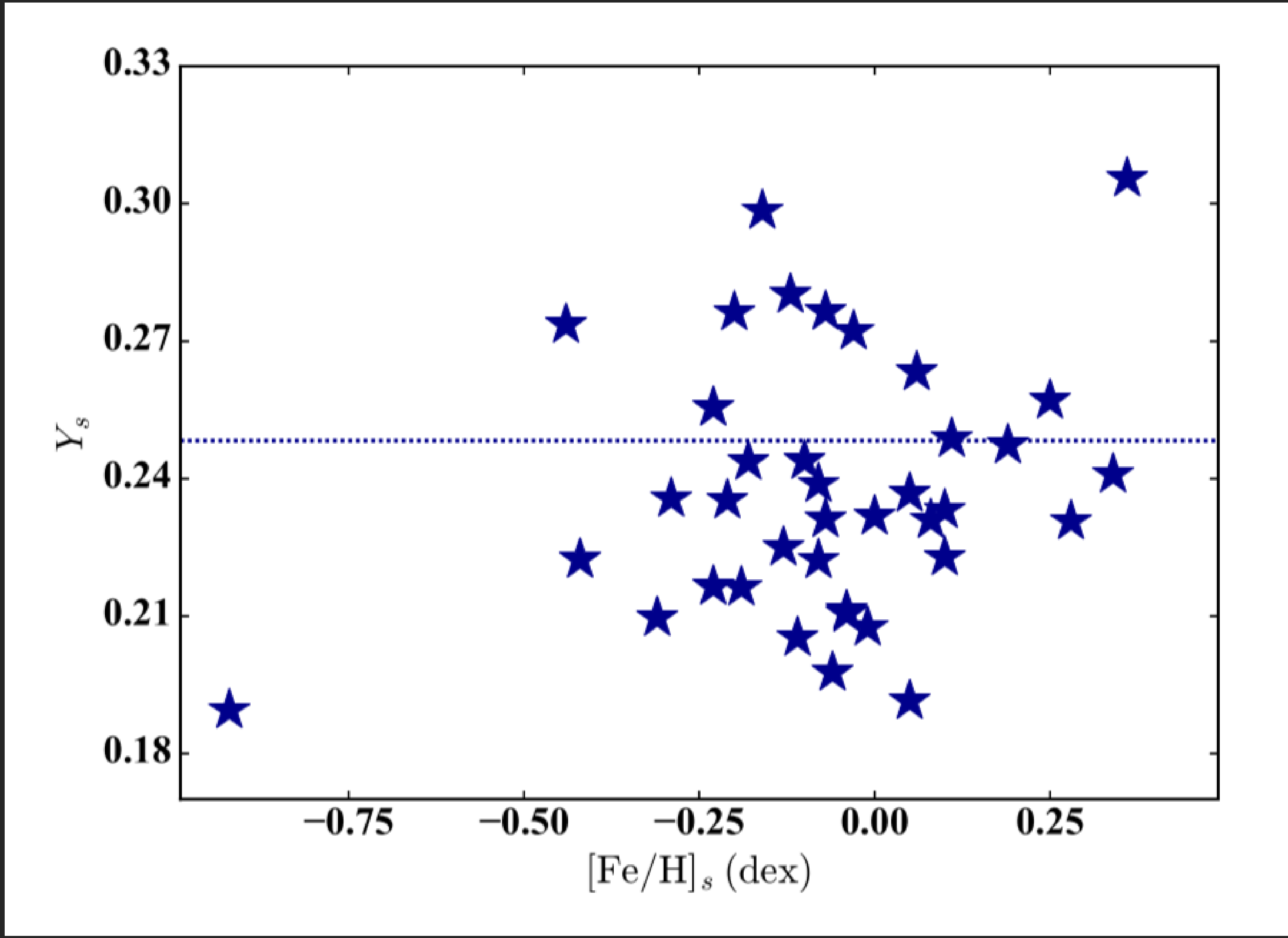

Fig 1.9

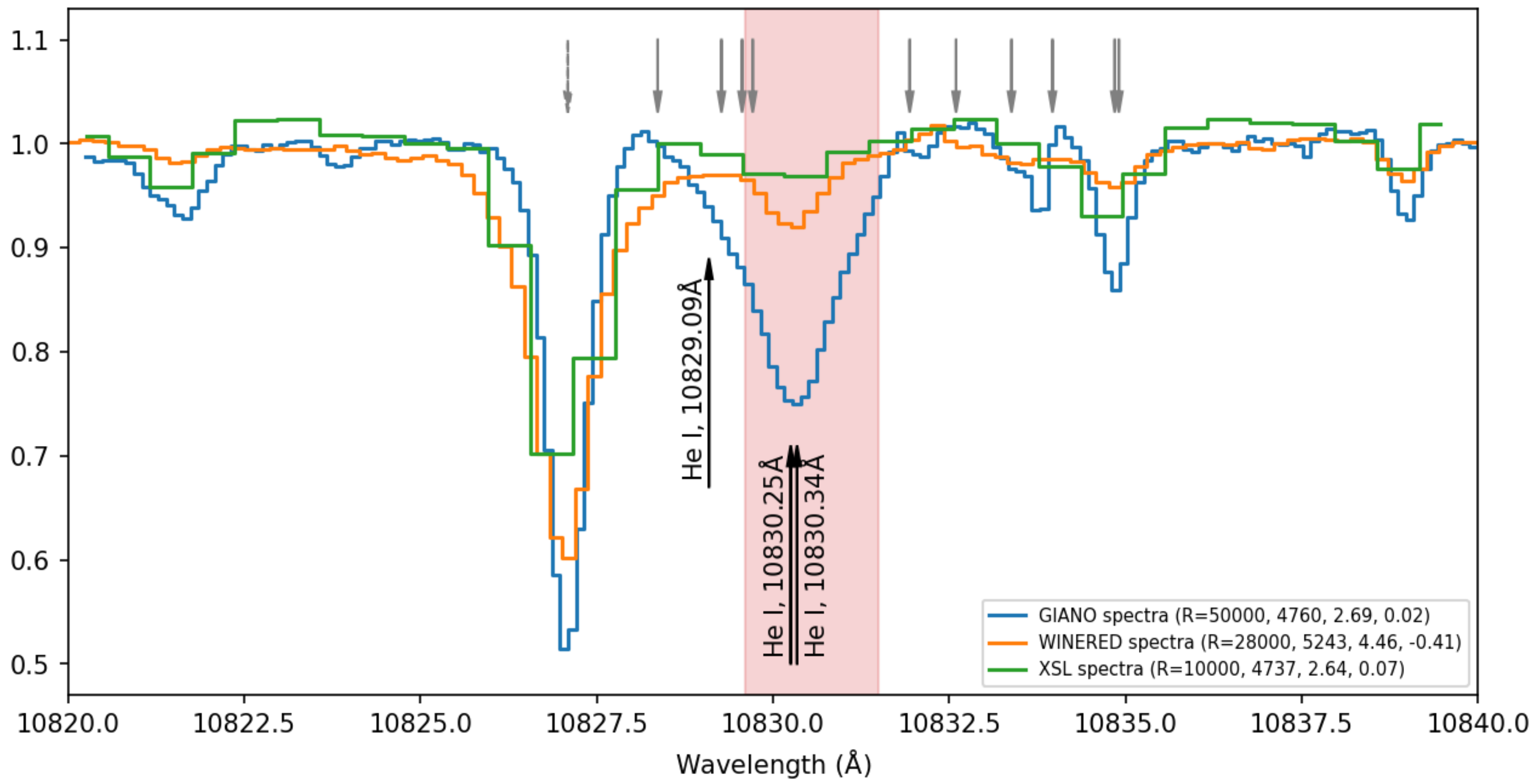

1.1
1.0
0.9
0.8
0.7
0.6
0.5
He I, 10829.09Å
He I, 10830.25Å
He I, 10830.34Å
GIANO spectra (R=50000, 4760, 2.69, 0.02)
WINERED spectra (R=28000, 5243, 4.46, -0.41)
XSL spectra (R=10000, 4737, 2.64, 0.07)
10820.0
10822.5
10825.0
10827.5
10830.0
10832.5
10835.0
10837.5
10840.0
Wavelength (Å)

Fig 2.4

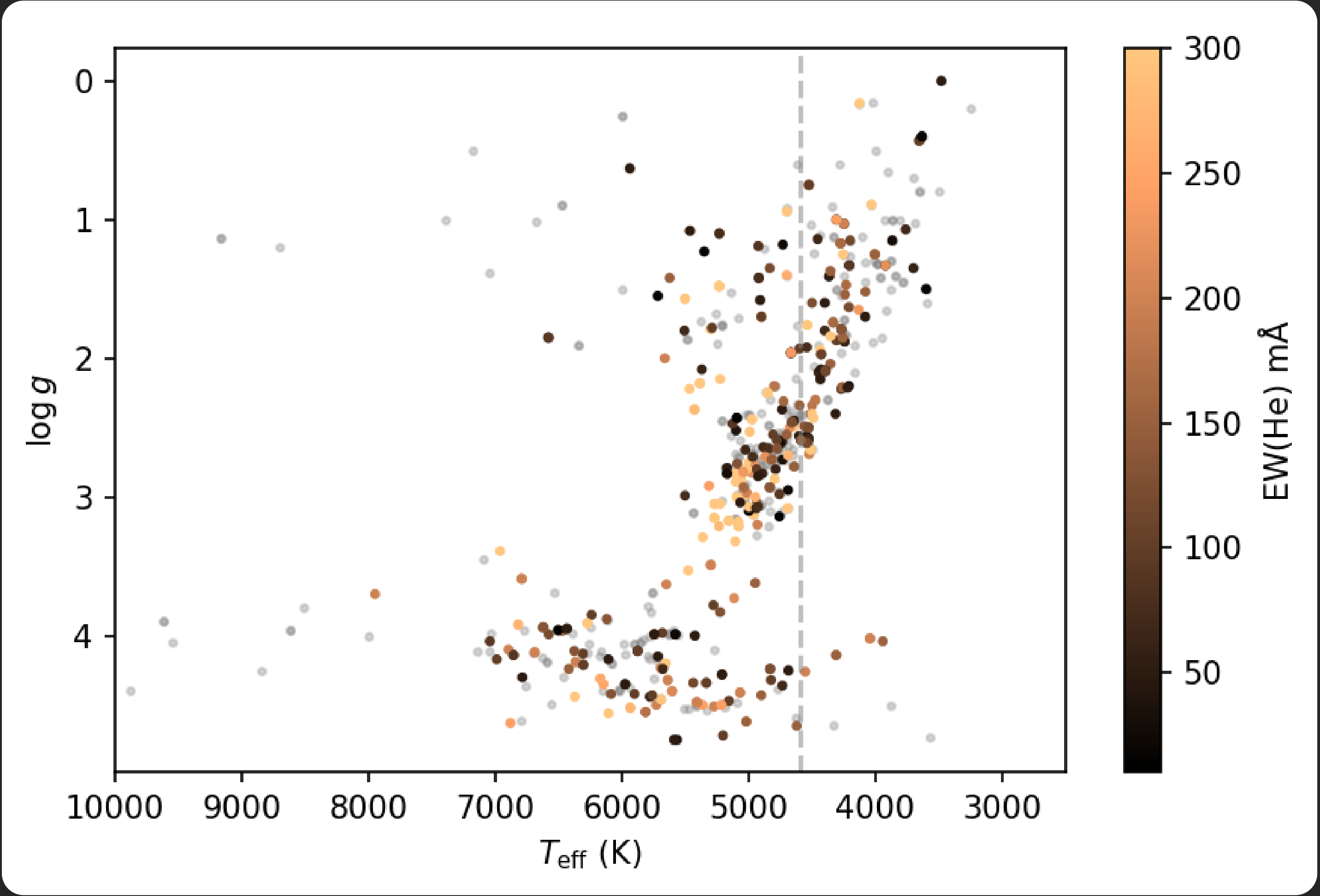

0
1
2
3
4
log g
10000
9000
8000
7000
6000
5000
4000
3000
T_{eff} (K)
300
250
200
150
100
50
EW(He) mÅ

Fig 2.7

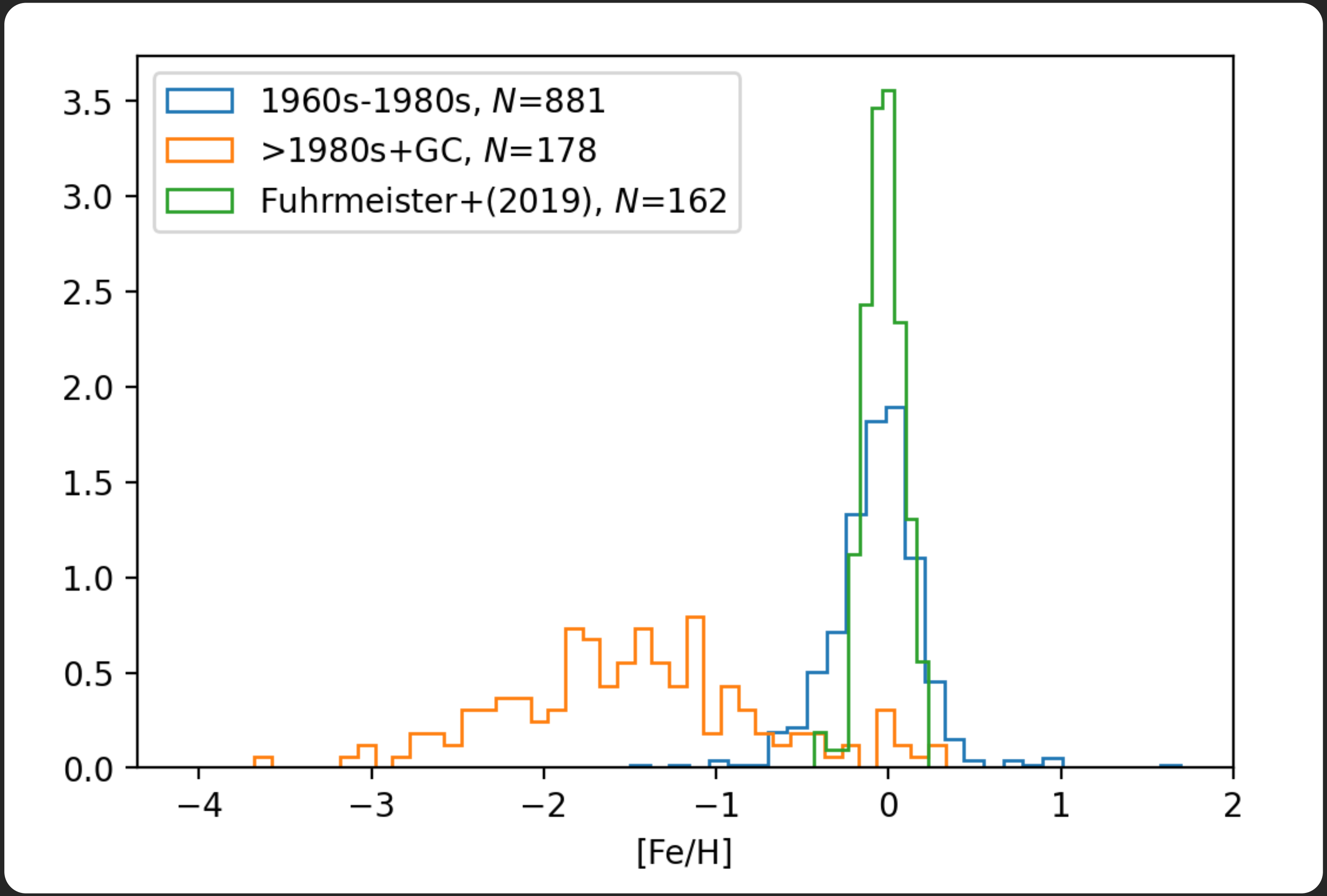

1960s-1980s, N=881
>1980s+GC, N=178
Fuhrmeister+(2019), N=162
3.5
3.0
2.5
2.0
1.5
1.0
0.5
0.0
−4
−3
−2
−1
0
1
2
[Fe/H]

Fig 5.1

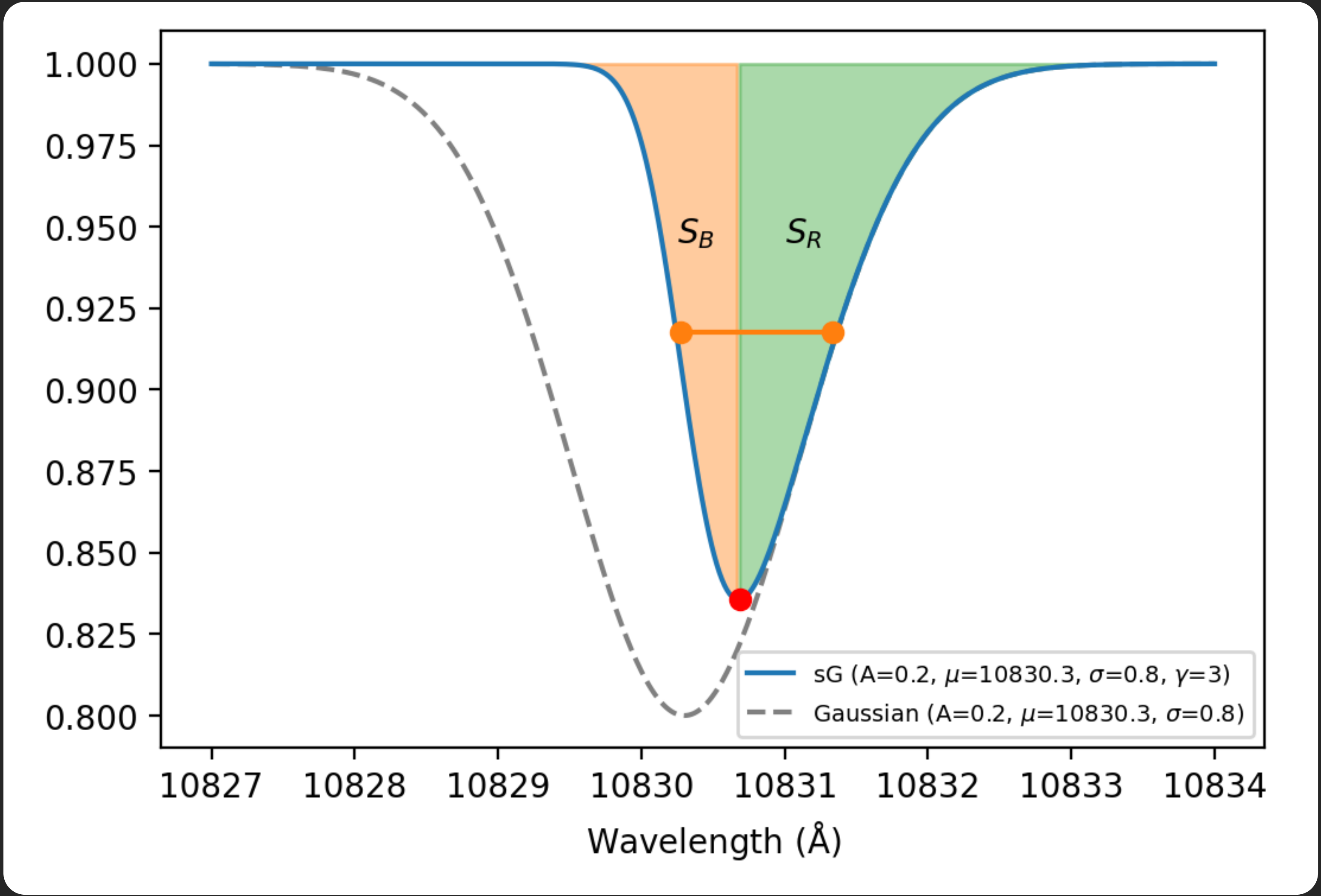

1.000
0.975
0.950
0.925
0.900
0.875
0.850
0.825
0.800
S_B
S_R
sG (A=0.2, μ=10830.3, σ=0.8, γ=3)
Gaussian (A=0.2, μ=10830.3, σ=0.8)
10827
10828
10829
10830
10831
10832
10833
10834
Wavelength (Å)

Fig 7.2

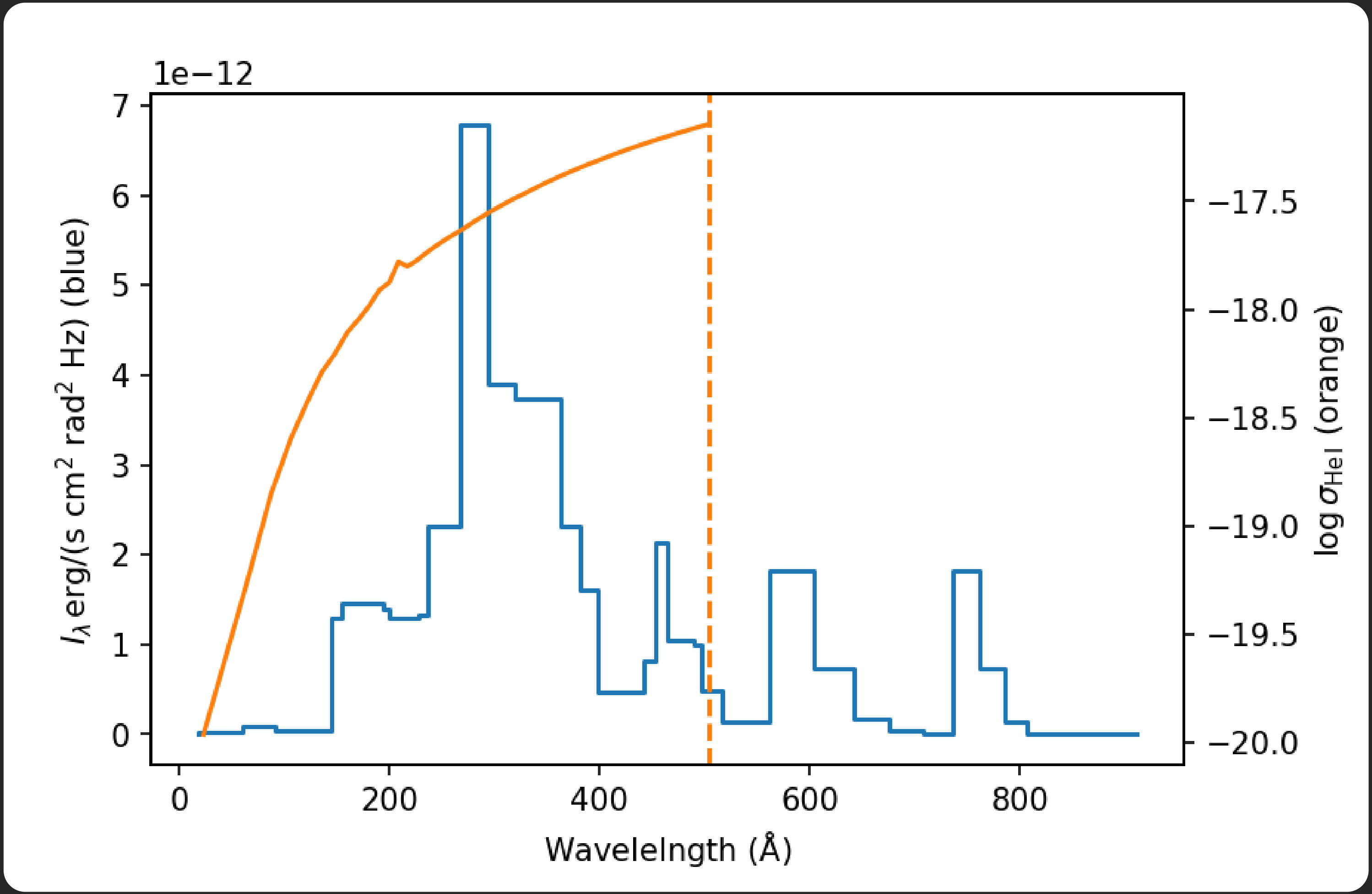
1e−12
7
6
5
4
3
2
1
0
I_λ erg/(s cm^2 rad^2 Hz) (blue)
0
200
400
600
800
Wavelelngth (Å)
−17.5
−18.0
−18.5
−19.0
−19.5
−20.0
log σ_{HeI} (orange)

Fig 7.9

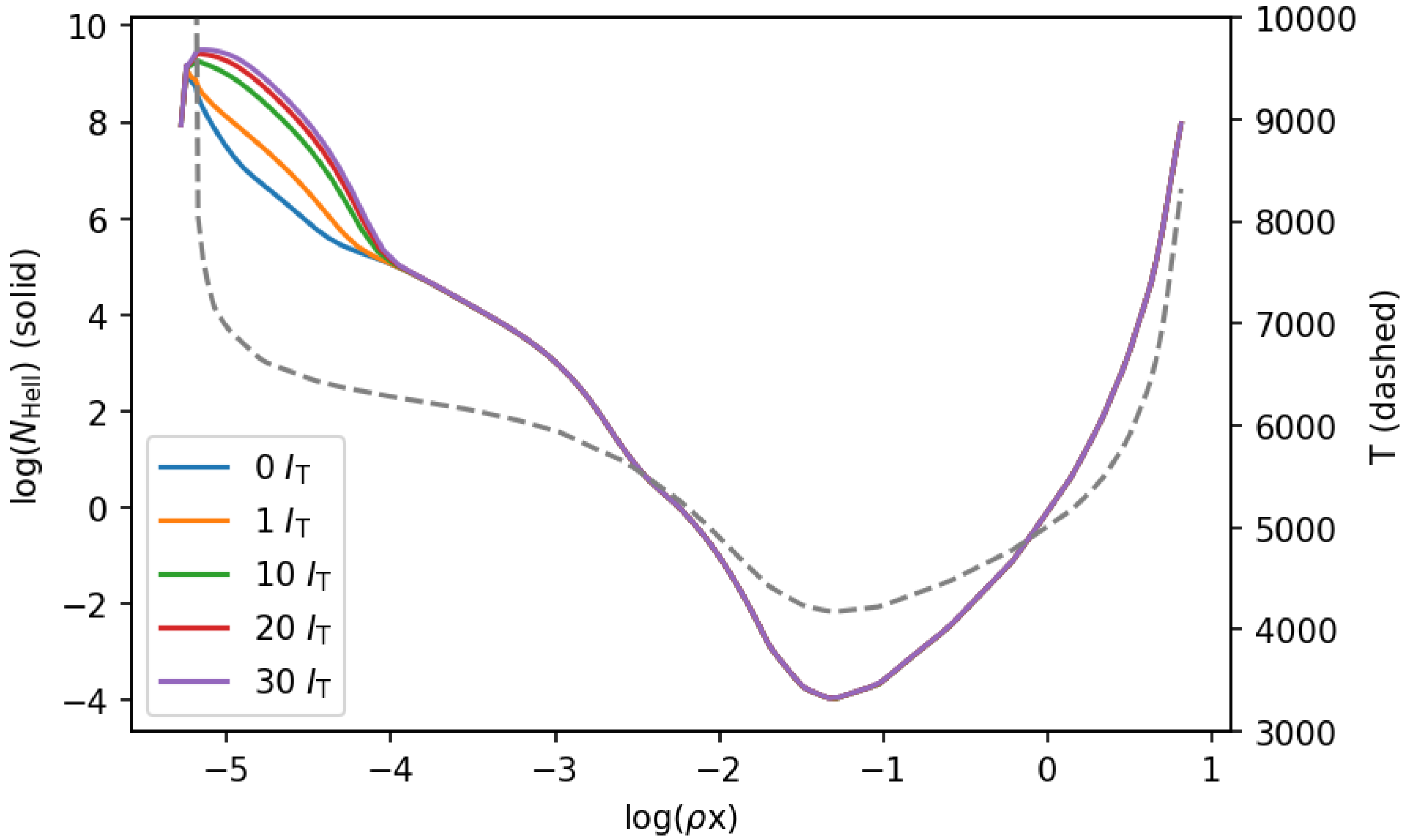

10
8
6
4
2
0
−2
−4
log(N_{HeII}) (solid)
10000
9000
8000
7000
6000
5000
4000
3000
T (dashed)
−5
−4
−3
−2
−1
0
1
log(ρx)
0 I_{T}
1 I_{T}
10 I_{T}
20 I_{T}
30 I_{T}

Fig 7.13

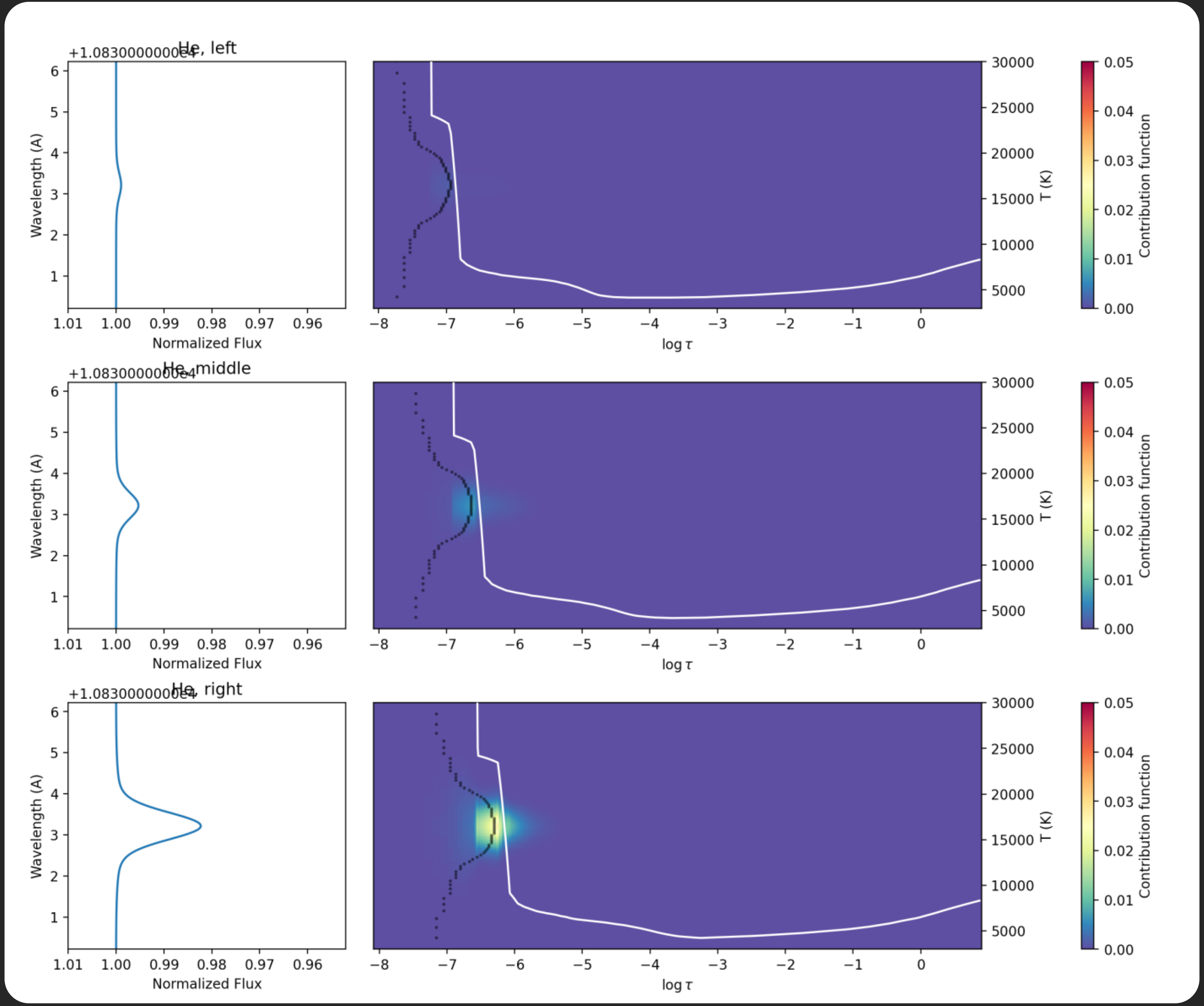

+1.0830000000e4 He, left
+1.0830000000e4 He, middle
+1.0830000000e4 He, right
Wavelength (A)
Normalized Flux
log τ
T (K)
Contribution function

Fig 8.4

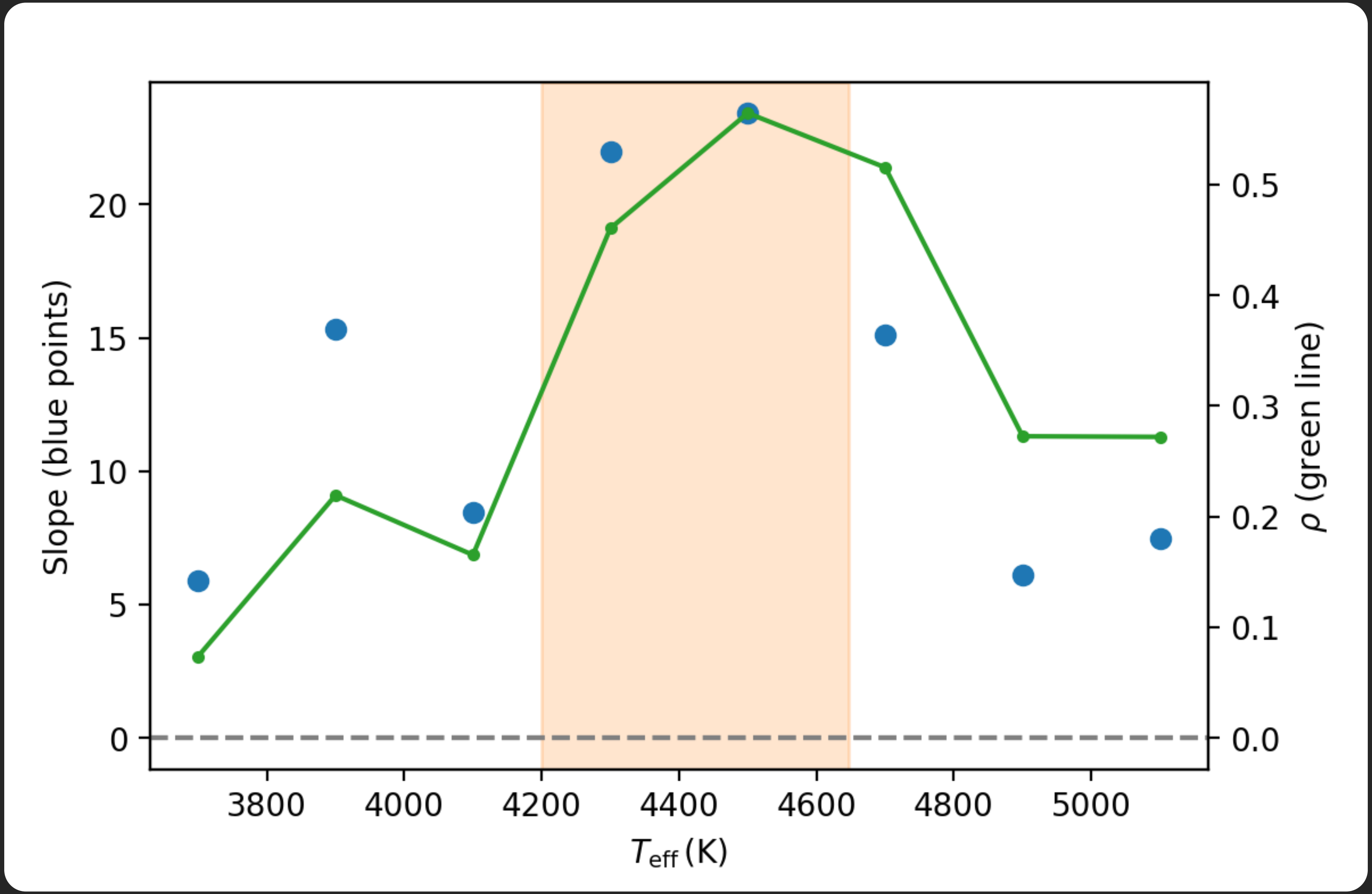

20
15
10
5
0
Slope (blue points)
0.5
0.4
0.3
0.2
0.1
0.0
ρ (green line)
3800
4000
4200
4400
4600
4800
5000
$T_{\rm eff}$ (K)